

СООБЩЕНИЯ
ОБЪЕДИНЕННОГО
ИНСТИТУТА
ЯДЕРНЫХ
ИССЛЕДОВАНИЙ
Дубна

800008

E13-2008-168

168-08

The ACCULINNA-2 Collaboration

FRAGMENT SEPARATOR ACCULINNA-2

Letter of Intent

394.10

Contents

1	Introduction	3
2	Status of the ACCULINNA fragment separator	3
2.1	Major accomplishments	4
2.2	International collaboration	5
2.3	Advantages of the ACCULINNA fragment separator	6
2.4	Need for further developments	7
3	Motivation for the new fragment separator	8
3.1	Scientific diversification	8
3.2	Standard instrumentation ideology	8
3.3	Scientific uniqueness	9
4	Anticipated scientific agenda	9
4.1	Nuclear reactions	11
4.1.1	Reaction mechanisms	11
4.1.2	Final state interactions and correlations	11
4.1.3	Production of intense radioactive beams and the neutron drip-line exploration	12
4.2	Nuclear structure	13
4.3	Astrophysical applications	14
4.3.1	Motivation	14
4.3.2	Nuclear matter properties for astrophysics	14
4.3.3	Nuclear data for astrophysics	15
4.3.4	Experimental methods for nuclear astrophysics	15
4.4	Elastic scattering	16
4.5	Inelastic scattering	17
4.6	Resonant elastic scattering	17
4.7	Transfer reactions	19
4.8	Coulomb dissociation	22
4.9	Knockout reactions and quasi-free scattering	24
4.10	Radioactive decays	27
4.10.1	Beta-delayed decays	27
4.10.2	Particle or cluster radioactivity	27
4.10.3	Novel experimental methods	28
4.11	Breakup reactions in general and continuum spectroscopy	29
4.12	Fusion-evaporation and incomplete fusion reactions	30

Объединенный институт
ядерных исследований
БИБЛИОТЕКА

4.13	Study of the quasi-fission reaction using in-flight separation	32
5	Proposed ACCULINNA-2 technical characteristics	36
5.1	The increase of the beam intensity	41
5.2	The beam quality improvement	42
5.3	Expected beam properties	42
5.4	Broadening of the experimental opportunities	43
6	Tentative timetable and cost estimates	44
7	Participants	44
8	References	45
9	Tables	54

1 Introduction

At present one of the principal fields of research at Flerov Laboratory of Nuclear Reactions (FLNR, Joint Institute for Nuclear Research, Dubna, Russia) is the Radioactive Ion Beam (RIB) research. This is conducted in the framework of the DRIBs initiative (Dubna Radioactive Ions Beams, <http://flerovlab.jinr.ru/flnr/dribs.html>). This document is the letter of intent for the construction of the in-flight fragment separator ACCULINNA-2 as the third generation of the DRIBs facilities. It should be constructed in parallel with continuous operation of ACCULINNA fragment separator and should gradually replace the latter after commissioning.

2 Status of the ACCULINNA fragment separator

ACCULINNA fragment separator is working with full load since 1996. The obtained scientific results are recognized by the nuclear physics community which is reflected by the list refereed publications and conference proceedings provided in the end of this Letter.

The heavy ion cyclotron U-400M (see Fig. 1 in page 33 for general view of the facility) was commissioned in 1992 and significantly upgraded in 2008. Initially, the fragment separator ACCULINNA was intended as an injector for the K4/K10 acceleration/storage complex [Yu.Ts. Oganessian *et al.*, *Z. Phys. A341* (1992) 217]. It was built out of magnets that were at hand from the spare set of the U-400M cyclotron beam lines and was commissioned in 1996. The first experiments at ACCULINNA (Ref. [2], <http://aculina.jinr.ru>) were performed in the autumn 1996 in the hall of the U-400M cyclotron (see Fig. 1). In 2000 the separator beam line was extended into the neighbouring low-background hall and equipped with a modern reaction chamber and unique cryogenic tritium target [13]. Since that time a series of precision experiments aimed at the study of the lightest neutron-rich isotopes ${}^{4,5,7}\text{H}$ and ${}^{6,7,8,9,10}\text{He}$ has been performed.

The ACCULINNA group actively works in all modes of operations typical for modern international centers:

- Numerous experiments are performed “in-house”; average workload is 3 – 4 months of the beam-time per year.
- The facility hosts external guest experiments.
- The group members actively participate in external experiments.
- The ACCULINNA group participates in the development of instrumentation for other world leading facilities in the field.

2.1 Major accomplishments

Within the recent years the ACCULINNA group has not only used recognized approaches to RIB research. It has proposed, developed, and practically applied a novel approach to the investigation of resonant states of nuclei in proximity and beyond the neutron dripline¹. The ACCULINNA group did not restrict the study of resonant states to the derivation of the invariant/missing mass spectra. It succeeded to show that, in the experiments performed with certain kinematical settings, correlations inherent to the reaction products become an extremely rich source of the information.

Unique technical feature of the ACCULINNA separator is the availability of tritium beams and cryogenic tritium targets. At the moment it is the only place in the world where the availability of the tritium target and the beam is combined with the RIB research. Within the operation time of ACCULINNA the following main results were obtained at this facility:

1. The dineutron and $t+t$ configurations in the structure of the ${}^6\text{He}$ neutron halo nucleus were experimentally established [3, 4, 6] as a result of measurements done in wide angular ranges for the elastic ${}^4\text{He}+{}^6\text{He}$ scattering and the ${}^6\text{He}+p \rightarrow {}^4\text{He}+t$ reaction cross sections.
2. For the first time the spectra of the ${}^3\text{H}({}^2\text{H},p){}^4\text{H}$ and ${}^3\text{H}({}^3\text{H},d){}^4\text{H}$ reaction products arising from the population of the ${}^4\text{H}$ ground state resonance were disentangled from events coming from different reaction mechanisms and the parameters of the ${}^4\text{H}$ ground state were reliably derived [18].
3. A lower limit for the ${}^7\text{H}$ decay energy was established in [17].
4. The ${}^5\text{H}$ spectrum has been reliably established. This result was achieved in a series of works [8, 12, 20, 21], in active polemics with the results coming from other groups.
5. Experimental methods for the analysis of the three-body decays of spin-aligned states were developed and applied [20, 21].
6. The ${}^8\text{He}$, ${}^9\text{He}$, and ${}^{10}\text{He}$ spectra were revised in [22] and [24]. Before these works, the low-lying spectra of these nuclei have been considered as reliably established for more than a decade.

Scientific results of experiments performed at the ACCULINNA fragment separator and the technical progress of the facility are reflected in about 50 publications (see the Reference section

¹In principle, one could consider this approach to be a combination of known experimental techniques. However, there is a specific combination of these techniques which was shown to be highly efficient for the RIB research.

at the end). Among publications there are papers in the leading refereed journals in the field: Physical Review Letters (3 papers), Physical Review C (4 papers), and Physics Letters B (6 papers). The technical progress of the fragment separator and instrumentation was reported in 7 publications in Nuclear Instruments and Methods.

2.2 International collaboration

The ACCULINNA group has a successful record of international collaboration. Particularly, for a long time mutually beneficial collaboration with GANIL (France), GSI (Germany), Kurchatov Institute (Russia), IPN Orsay (France), RIKEN (Japan), Texas A&M University (USA), Warsaw University (Poland), and other scientific centers is taking place. This activity is indicated in numerous common works (see Refs. [6, 8, 9, 10, 11, 12, 13, 14, 18, 19, 20, 21, 22, 24, 25]) and INTAS Grants Nos. 03-51-4496 and 05-100000-8272.

1. The members of the group participated in the design work on the VAMOS spectrometer (<http://www.ganil.fr/vamos/projdes.html>) and modernization of the active gas target MAYA [34, 35] at GANIL, at the moment some of the group members are involved into the new projects ACTAR, PARIS and GASPARD developed in the framework of SPIRAL2 (<http://www.ganil.fr/research/developments/spiral2/collaborations.-html>).
2. Current and future collaborations with GSI are mainly defined by the participation in the NUSTAR projects R3B/EXL/ELISE at FAIR (<http://www.gsi.de/fair/reports/index.html>). In particular, the ACCULINNA staff is responsible for the R&D, design and tests of a scintillator shell of the R3B/EXL calorimeters and in-ring instrumentation for ELISE.
3. In the framework of the FLNR-RIKEN collaboration several successful experiments were performed at ACCULINNA and RIPS separators [6, 8, 9, 10, 11, 12, 13, 14, 18, 19, 20, 21, 22, 24, 25]; new proposals for the BigRIPS experiments were put forward (<http://www.-nishina.riken.jp/Eng/facilities/RIBF.html>).
4. Experiments proposed by the Notre Dame and Texas A&M University groups were performed in 2002, the results are reported in Ref. [15].
5. The time-of-flight neutron spectrometer DEMON (<http://ireswww.in2p3.fr/ires/recherche/demon/demon.htm>) was several times used in experiments performed in Dubna jointly by the groups of ACCULINNA, ULB (Brussels), IRS (Strasbourg), and GANIL [10, 12, 18, 20, 21, 24, 25].

6. Recently experiments aimed at the study of complete and incomplete fusion of ${}^6\text{He}$ and ${}^6\text{Li}$ projectile nuclei interacting with medium mass targets were performed in collaboration with the groups of CSNSM (Orsay), IRS (Strasbourg), ULB (Bruxelles), Vanderbilt University (Nashville, Tennessee) and iThemba LABS & Stellenbosch University (South Africa).
7. The ACCULINNA group and the nuclear physics group of Vanderbilt University (Nashville, Tennessee, USA) achieved a number of new, significant results in their long-term collaborative study of the ${}^{252}\text{Cf}$ spontaneous fission. These include the first time measurements of the independent yields of around 200 fragment pairs emitted in the spontaneous fission, the new measurements of the fission fragment angular momentum values, the new data characterizing ternary fission of ${}^{252}\text{Cf}$ (e.g., the yields of the ${}^{10}\text{Be}$ cluster in the ground state and 2^+ excited state were measured and the pre-scission temperature in the neck was estimated for the first time). The number of joined papers published on these topics in refereed journals exceeds 100 [J.H. Hamilton *et al.*, Prog. Part. Nucl. Phys. **38** (1997) 273; G.M. Ter-Akopian *et al.*, Phys. Rev. C **55** (1997) 543], see also <http://aculina.jinr.ru/cf252.htm>.
8. A novel time-projection chamber design has been recently developed at Warsaw University for studies of correlations in extremely rare decays. This chamber was tested at ACCULINNA in the experiment on β -delayed particle emission for ${}^{12}\text{N}$ and ${}^{13}\text{O}$ [23].

2.3 Advantages of the ACCULINNA fragment separator

Thus, having the modest technical base and low expenses the ACCULINNA separator delivers important novel results. How the success of this project could be developed? First of all, it is necessary to outline what was the source of the interesting physics results obtained at this facility. The following factors should be emphasized:

1. The record intensity of the primary cyclotron beams (e.g., 3 – 10 p μ A of ${}^{11}\text{B}$).
2. Comparatively low (compared to the other in-flight separators) beam energy. This provides prerequisite for quite a good energy resolution in the measurements done in different experimental conditions. Relatively high reaction cross sections corresponding to the low beam energies accessible at ACCULINNA partly compensate for the low intensities of secondary beams.
3. The energy range of exotic beams provided by ACCULINNA is optimal for the nuclear structure studies done by means of transfer reactions. Due to the transparent reaction

mechanism this class of reactions is well understood and clear explanation becomes available for the data obtained in such experiments.

4. Complete kinematical measurements are performed routinely. As a result very clean, background-free spectra are obtained.
5. Essential consequence of such correlation measurements is the possibility of unambiguous spin-parity identification for the observed resonance states. The choice of kinematical conditions selecting specific reaction mechanisms (i.e., direct transfers, quasi-free scattering, spin alignment in zero geometry transfers) simplifies the data interpretation.

2.4 Need for further developments

Within the years of the ACCULINNA operation, the need for the further development of the in-flight RIB separation technique based on the primary beams delivered by the U-400M cyclotron became obvious.

1. The existing separator with one stage RIB cleaning is efficient only for the lightest neutron-rich nuclei. It does not cope with the request of high intensity clean beams of very neutron-rich and very proton-rich nuclei with atomic numbers $Z > 8$. E.g., for the proton-rich nuclei, the contamination level in the secondary beam is too high for efficient operation.
2. The large emittance of the secondary beams obtained from the relatively low energy primary beams provided by the U-400M cyclotron conflicts with the small acceptance of the existing separator. This leads to severe limitations in the intensity of the most exotic beams. Such RIBs of the prime interest as ^{11}Li , ^{14}Be , ^{17}B , ^{19}B , ^9C , ^{13}O , ^{17}Ne , etc. are available now only with very low intensities.
3. More powerful detector arrays are required for efficient measurements of multiple-coincidence events. The existing experimental area becomes too small to hold all the needed equipment. This imposes restrictions on the instrumentation positioned upstream (e.g., extra focusing elements) and downstream the reaction chamber (e.g., wide aperture arrays for neutron TOF measurements, set-up for detecting reaction products flying close to zero angle, etc.).
4. The small length of the separator imposed the major limitations on the energy resolution in many experiments: the final resolution is largely defined by the resolution attainable in the measurement of the incoming beam energy. The energy resolution is limited now mainly by the short TOF base.

3 Motivation for the new fragment separator

Evidently the next generation facility should enhance the advantageous features of the existing facility and eliminate/diminish the disadvantages as much as possible. The next generation fragment separator is expected to be a more universal and powerful instrument. The beam intensity should be increased, the beam quality improved, and the range of the accessible secondary radioactive beams broadened.

3.1 Scientific diversification

On the one hand, ACCULINNA has furnished excellent conditions for progress in the studies of the super-heavy hydrogen and helium isotopes. On the other hand, diversification of research program carried out at this facility is needed. In the long-time prospect it is not acceptable that the whole research at the facility is only focused on the reactions involving several nuclei². The proposed development of the ACCULINNA-2 fragment separator suggests a more universal scientific instrument giving a variety of clean and well-prepared secondary beams limited only by choice of the primary beams provided by the U-400M cyclotron.

3.2 Standard instrumentation ideology

An important task of the ACCULINNA-2 project is the realization of the beam usage concept at FLNR complying with the modern trends inherent to large RIB facilities.

The fragment separator, together with the beam diagnostics system, should become a *standard instrument* for the laboratory. The idea is that the exotic beam is delivered for the users into the low-background experimental area with full particle-by-particle identification and (energy/angle) diagnostics. Nowadays, such an approach is standard at the large international RIB facilities. The ultimate purpose is that the secondary beam users should not worry about the incoming beam at all. This facilitates the RIB use by different groups running various experiments.

The development of new detector systems and mastering modern digital technologies for the ACCULINNA-2 project include:

1. Zero angle spectrometer for the detection of beam-like reaction products in the case of high beam intensity.

²It does not mean that the reaction studies with heavier neutron-rich and even proton-rich RIBs are not possible at ACCULINNA, but such experiments would experience considerable difficulties which hinder the above mentioned advantages of the ACCULINNA facility and will not allow high-class scientific results.

2. Beam tracking detectors based on the micro-strip silicon/diamond detectors.
3. Micro-strip silicon or/and diamond detectors providing a very good time resolution ($\sigma \sim 50$ ps) for TOF measurements.
4. Neutron detector arrays based on the toluylene crystals and conventional multi-layer plastic scintillator arrays.
5. Arrays of CsI, LaBr₃, etc. crystals for charged particle detection and Ge γ -ray detector arrays.
6. Universal DAQ MBS (Multi Branch System) capable to combine the main standards of digital electronics modules (CAMAC, Fastbus, VME, VXI).

3.3 Scientific uniqueness

The ACCULINNA-2 facility is not intended to compete with the new large in-flight RIB facilities (SuperFRS at FAIR, A1900 at MSU, or RIPS at RIKEN, see Table 1) in the sense of “crude power”. It should complement the existing/constructed facilities in certain fields. Namely, ACCULINNA-2 should provide high intensity RIBs in the lowest energy range attainable for the in-flight separators. We emphasize scientific importance of this specific field of research and consequently we choose a cost-effective technical solution for this project. Within a minor fraction of the price of the modern RIB facilities (the estimated cost of the ACCULINNA-2 project is ~ 8 M\$, see Section 6) it is possible to pursue world-class research due to a *specific scientific focus* of this instrument. The prime objectives of ACCULINNA-2 are to provide *a good energy resolution* for the beams of radioactive nuclei and high efficiency for *correlation measurements*. The later, combined with the selection of certain reaction mechanisms and the choice of specific kinematical conditions, could provide the spin-parity identification. In that case, the relatively low-energy secondary beams will provide for ACCULINNA-2 a unique position among other fragment separators³.

4 Anticipated scientific agenda

Research with radioactive beams is one of the most important modern trends in nuclear physics. The investigation of nuclei far from β -stability valley and even beyond the nuclear stability lines is important for understanding the properties of nuclear matter at the extreme conditions. It is also necessary for the further development of nuclear theory and indispensable for nuclear

³So far, the energies in a range of 10 – 40 MeV/amu are not available at other large-scale in-flight RIB separators.

astrophysics. The new dripline nuclear physics intertwines the nuclear structure and reaction mechanisms more than ever before.

The proposed ACCULINNA-2 project is focused on the study of nuclear properties far from the stability valley. Near the proton or neutron drip-lines the lowest nucleon and cluster thresholds become close to the ground state (evidently, beyond the drip-lines these thresholds are below the ground state). Close to the thresholds clusterization phenomenon becomes increasingly important: some states possess expressed cluster structures and new forms of nuclear dynamics arise. Among these the following should be mentioned:

- Nucleon haloes (neutron skins, Efimov states, etc.).
- Soft excitation modes (e.g., the soft mode of the giant dipole resonance).
- New magic numbers and intruder states.
- Two-proton radioactivity (few-body decays in more general terms).

The research focused on nuclear astrophysics and the novel forms of nuclear dynamics presumes dedicated scientific program, high intensity beams, and specialized instrumentation suitable for precision measurements.

There are two ways to overview the scientific agenda:

- We can look at the scientific agenda from the side of the *physical problems*. The main broad physical topics are:
 - Nuclear reactions.
 - Nuclear structure.
 - Astrophysical applications.
- Each major research direction has a preferable set of methods by which its problems could be best handled. Therefore, another way to look at the scientific agenda of the ACCULINNA-2 separator is to consider *physical methods* to study the properties of the nuclear systems which should be accessible with this instrument. It is clear that the same experimental methods can be used to resolve different physical questions with smaller or larger success. ACCULINNA-2 is proposed to become a versatile instrument with broad range of accessible methods:
 - Elastic scattering.
 - Inelastic scattering.
 - Resonant elastic scattering.
 - Transfer reactions.
 - Coulomb dissociation.
 - Breakup reactions in general and the spectroscopy of a continuum.

- Knockout reactions and the quasi-free scattering.
- Radioactive decays.
- Fusion-evaporation and incomplete fusion reactions.

Below we give a brief overview of prospective applications of the ACCULINNA-2 facility in view of this broad scientific agenda. General points are illustrated by examples (contained in frames) of especially interesting research performed either at ACCULINNA or at other RIB facilities.

4.1 Nuclear reactions

Nuclear reactions are among the most efficient tools⁴ of nuclear research and one of the most important possibilities to get an information on nuclei far from stability lines. Simultaneously, they are the subject of investigation by themselves. Quite often clarification of the reaction mechanism could be indispensable for correct interpretation of the obtained data: appropriate choice of the energy and kinematical conditions can lead to significant simplifications. For reactions with several fragments in the final state the Final State Interaction (FSI) could influence observables drastically. The in-flight RIB separation, by itself, needs an intimate knowledge of the fragmentation reaction mechanisms to arrive at the efficient operation of the separator.

4.1.1 Reaction mechanisms

When we are interested, e.g., in the information on the nuclear structure, the impact of the reaction mechanism to the results of measurements should be well understood and reliably disentangled from the information of interest. Below we illustrate this point by the example of studies of the ^{10}He nucleus. The situation with this system remains quite puzzling. Without clarification of the reaction mechanism these data (which have low statistics) should have been simply useless.

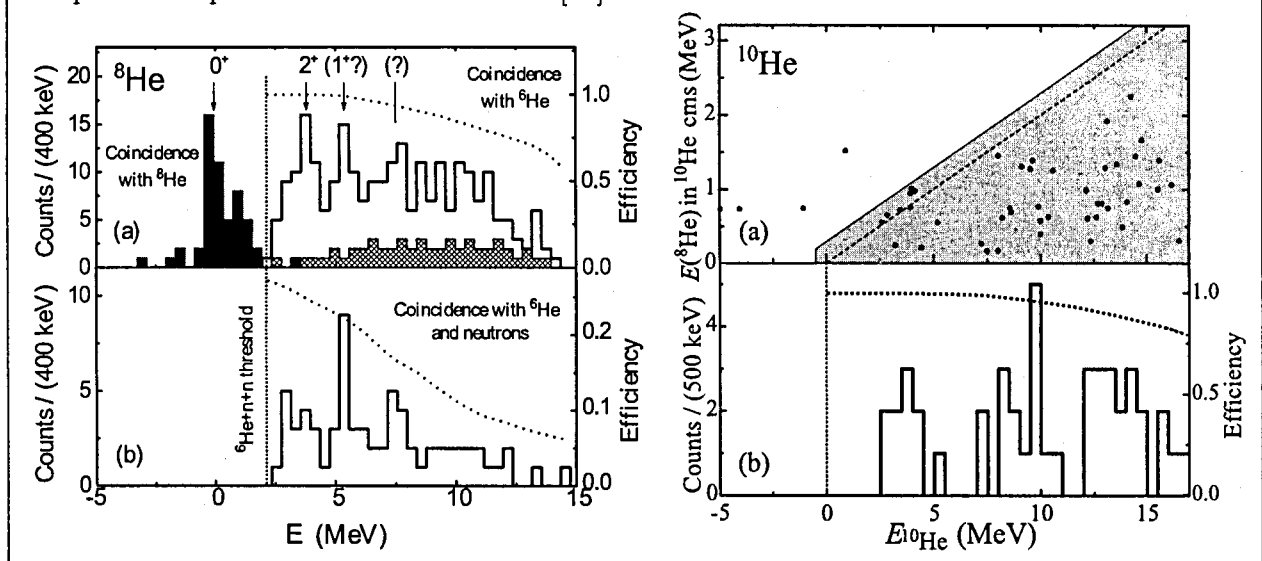
4.1.2 Final state interactions and correlations

In the reactions leading to fragmentation or decay of the nuclear system, the momentum distributions among the decay fragments should, in principle, contain some information about momentum distributions in the initial system. Important effect masking this information is interaction of fragments in the final state. A simple approximation in which this effect can be

⁴Electromagnetic and weak probes are much more reliable tools in the sense of the theoretical interpretation of the obtained results. However, weak processes give access only to a narrow subset of possible information; such an approach as the electron scattering on stored RIBs has a limited applicability in the sense of the nuclear lifetimes. It is planned to be realized at the next generation of RIB facilities.

taken into account for two particles is the Migdal-Watson approach. More precise treatment of the problem could be a theoretical problem. Complicated reactions, especially with nuclei near the driplines, could lead to more than two fragments in the final state. There is no good understanding of FSIs among three or more fragments. Development of this field would require considerable effort from both theory and experiment (see also some discussion in Section 4.11).

Example: The excitation spectra of ${}^8\text{He}$ and ${}^{10}\text{He}$ were studied in the ${}^6\text{He}(t,p){}^8\text{He}$ and ${}^8\text{He}(t,p){}^{10}\text{He}$ reactions [24]. Both reactions were performed at close energies and at similar kinematical conditions. For that reason the ${}^8\text{He}$ spectrum can be used for “calibration” of the ${}^{10}\text{He}$ data. The ground state ${}^{10}\text{He}$ peak was not observed at the expected energy around 1 MeV. Although the statistics of the ${}^{10}\text{He}$ spectrum is very low, this fact is significant. Using the appropriate theoretical arguments we can find that at least 8 of the ${}^{10}\text{He}$ events should have been observed in the ground state region. Probability of the situation that the ground state is at 1 MeV but not populated by chance due to statistics only is about 10^{-4} . Thus we arrive at a conclusion that either the real ${}^{10}\text{He}$ g.s. position is about 3 MeV or the reaction mechanisms are drastically different for the ${}^6\text{He}(t,p){}^8\text{He}$ and ${}^8\text{He}(t,p){}^{10}\text{He}$ reactions, what is quite unexpected. Situation here remains unclear; other possible explanations can be found in [24].



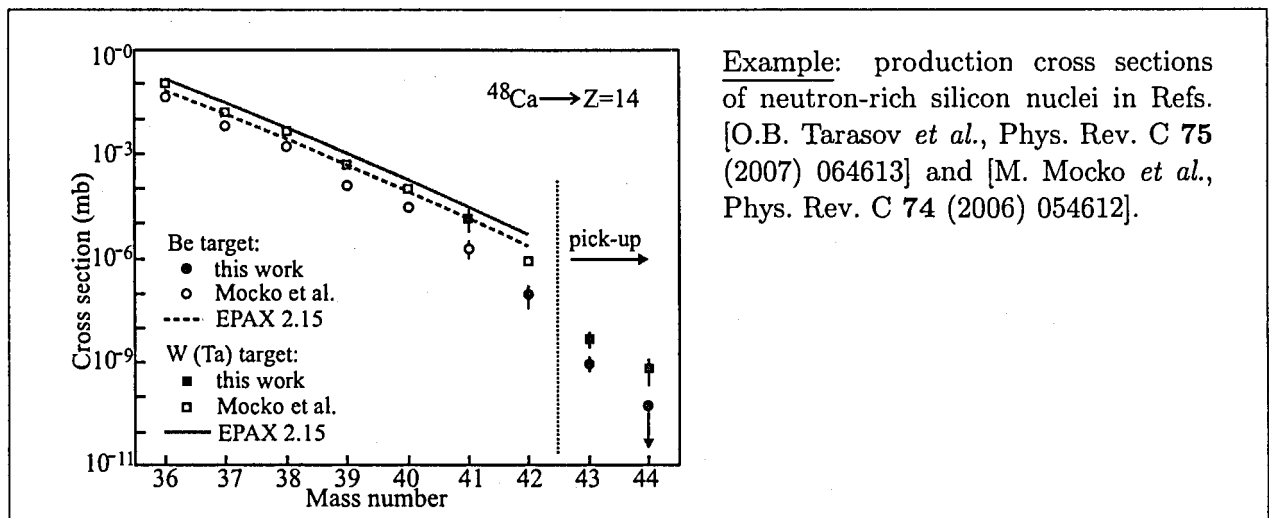
4.1.3 Production of intense radioactive beams and the neutron drip-line exploration

The study of reaction mechanisms is an important approach both to testing nuclear models and planning experiments with secondary beams. In the energy domain (20 – 50 MeV/amu) where the velocity of incident beam nuclei becomes comparable with the Fermi velocity of nucleons in the nucleus, many experiments have shown that the production of fragments may occur through several competing processes of multi-nucleon transfer reactions. So, in a recent MSU experiments [O.B. Tarasov *et al.*, Phys. Rev. C **75** (2007) 064613. T. Baumann *et al.*, Nature (London) **449** (2007) 1022] the new neutron-rich isotopes ${}^{44}\text{Si}$, ${}^{42,43}\text{Al}$ were produced through

the transfer reactions taking place at a beam energy of 140 MeV/amu. These experiments have shown the importance of the target choice for obtaining optimum production rates for exotic nuclei (see example below). It was demonstrated that the neutron-rich tails of the obtained isotope distributions have a linear dependence similar to the Q_{gg} systematics ascertained for the low-energy two-body reactions.

Large acceptance of the new fragment separator will allow to increase at least by a factor of 10 the exotic beam intensities and approach the neutron drip-line where the choice of the production reaction becomes crucial.

The production of nuclei along the neutron drip-line provides a benchmark for testing the existing nuclear mass models. The determination of the true cross sections is important for improving models allowing one to better estimate the feasibility of certain experiments in this region.



Example: production cross sections of neutron-rich silicon nuclei in Refs. [O.B. Tarasov *et al.*, Phys. Rev. C 75 (2007) 064613] and [M. Mocko *et al.*, Phys. Rev. C 74 (2006) 054612].

4.2 Nuclear structure

Here we briefly discuss the major topics of the nuclear structure research and consider whether they are accessible at the proposed facility.

- Energies, widths, and spin-parities of nuclear states. ACCULINNA-2 facility should be especially efficient for the studies of nuclei in proximity and beyond the dripline. Studies of energies and widths should be facilitated by the improved energy resolution (see Section 5.2). Spin-parity identification for the particle (cluster) unstable states can be provided by correlation studies.
- Clusterization properties of the nuclei. Spectroscopic factors of nuclear states with respect to nucleons and clusters. These characteristics could be accessed at ACCULINNA-2 by elastic/inelastic scattering, quasifree scattering, or knockout reactions. The latter becomes reason-

able for the upper part of the beam energy range planned for ACCULINNA-2.

- “Geometric” information: nuclear sizes and shapes. The size information is best obtained in high-energy reactions, which are not the domain of the facility.
- Neutron and proton densities; neutron and proton radii. Limited information of this kind can be obtained by studies of the optical properties of various reactions with nuclei of interest.
- Correlations among nucleons and clusters in nuclei. This information can be obtained by studies of correlations in the decays of resonances or correlations of residues for the knockout.

We can see that a broad variety of the nuclear structure research topics is accessible at the proposed ACCULINNA-2 facility.

4.3 Astrophysical applications

4.3.1 Motivation

Nowadays the nuclear astrophysics research is an integral part of scientific work both at the major RIB “factories” and relatively small facilities. This research includes systematic improvement of the reaction data base, broadening the available mass and energy level data set. It is very important to carry out focused, dedicated investigations of some special cases being difficult for the experimental study but crucial for the stellar burning cycles.

Nuclear astrophysics benefits in several ways from the investigation of far-from-stability nuclei where the major aspect is new information on the nuclear matter properties and relevant nuclear reactions.

4.3.2 Nuclear matter properties for astrophysics

For understanding the late stages of stellar evolution (neutron stars and their life-cycle) the knowledge about the properties of infinite nuclear matter in various conditions (equation of state) is required. At the moment, theory cannot reliably bridge the gap from the nucleon-nucleon interaction, known in fine details, to the properties of infinite nuclear matter. Finite nuclear matter (namely, nuclei) is therefore the only directly accessible test bench for theoretical models. At the moment the situation is such that the results provided by different models are stable in the regions close to the β -stability valley and deviates from each other and from experiment when the driplines are approached. The further the experimental knowledge is extended beyond the dripline, the more precise testing and tuning of theoretical models is possible in this field.

Example: in the recent studies of the heavy helium isotopes at the ACCULINNA fragment separator the low-lying spectra of ^8He , ^9He , and ^{10}He were considerably revised. The improved ground state energy positions in ^9He and ^{10}He were found to be higher by ~ 0.7 MeV and ~ 1.5 MeV, respectively, than it was known before. From the theory side, it is interesting to note that the previously known positions of these states were well reproduced by several theoretical models.

4.3.3 Nuclear data for astrophysics

The calculations of the stellar burning cycles in astrophysical environments where the r-process or rp-process take place require massive data inputs for nuclei far from stability. Any thermonuclear burning cycle consists of a sequence of radiative capture reactions followed by weak decays (β^\pm or electron capture). Some cycles include reactions (N, α) or (α, N) as well. The required data can be classified as follows:

- Masses and level schemes in proximity of the neutron, proton, and alpha breakup thresholds.
- Weak decay lifetimes (β^\pm , electron capture).
- Partial proton, neutron, α , γ widths of low-lying resonances to calculate *resonant* radiative capture and (N, α) or (α, N) reaction rates
- The electromagnetic E1 and E2 strength functions to calculate *nonresonant* radiative capture. These strength functions can be reliably extracted from the data on the electromagnetic dissociation of corresponding nuclei in broad energy range and used for calibration of theoretical calculations in the extreme low energy range important for astrophysics.

4.3.4 Experimental methods for nuclear astrophysics

There are two major problems that nuclear physicists have to deal to determine stellar reaction rates. (1) Many nuclear reactions in stars involve two charged nuclei. At low stellar energies, the Coulomb repulsion between colliding nuclei makes reaction cross sections so small that in most cases it is impossible to measure them directly in terrestrial laboratories. (2) Most nuclear reactions in stars involve short-lived proton-rich and neutron rich nuclei that can be studied only with radioactive beams. The (n, γ) reactions are particularly difficult to study because neutrons are radioactive and short-lived target do not exist. Not all beams necessary for these purposes are easily available. So, in many cases, the cross sections of interest must be studied indirectly by other methods. The most actively used indirect methods are:

- Resonance reactions in inverse kinematics on hydrogen and helium targets.
- Transfer reactions to determine level schemes and spectroscopic properties of nuclear states. This includes peripheral transfer reactions to measure the quantities called Asymptotic Nor-

malization Coefficients (ANCs) that determine stellar capture that occurs at large separations between target and projectile.

- Electromagnetic dissociation as a reverse process to the radiative capture reaction.
- “Trojan horse” type reactions. They proceed in a presence of a third nucleus which behaves as a spectator.

Example: The cross sections of a radiative capture reaction (p, γ) often depends only on a single structure quantity called asymptotic normalization coefficient (ANC). They determine absolute value of the proton bound state wave function beyond the range of the strong interaction. The ANCs are usually measured using peripheral transfer reactions. A fresh idea in this field is to measure ANC not for the $p+(N, Z)$ state (which could be, e.g., technically problematic), but for the “isobaric” $n+(Z, N)$ reaction (when it is easier) [N.K. Timofeyuk *et al.*, Phys. Rev. Lett. **91** (2003) 232501]. This involves neutron transfer reactions. The most simple of them, the (d, p) reaction, often contains contributions from the internal part of the $n+(N, Z)$ wave function and the deuteron breakup contribution, which does not let the ANCs to be determined accurately enough. It would be more beneficial to use the (t, d) reaction which is peripheral in many cases and well suited to the ANC studies. For example, the solar ${}^7\text{Be}(p, \gamma){}^8\text{B}$ reaction can be investigated by means of the ${}^7\text{Li}(t, d){}^8\text{Li}$ reaction, the rp-process reaction ${}^{42}\text{Ti}(p, \gamma){}^{43}\text{V}$ can be investigated by means of the ${}^{42}\text{Ca}(t, d){}^{43}\text{Ca}$ reaction. Here, the cryogenic tritium targets and triton beams give an exclusive advantage to ACCULINNA and proposed ACCULINNA-2 facility.

4.4 Elastic scattering

A well known and relatively easy way to access data on nuclear sizes is via the “optical” properties of the projectile-target interaction. An example presented below illuminates this point by the example of the ${}^6\text{He}$ nucleus.

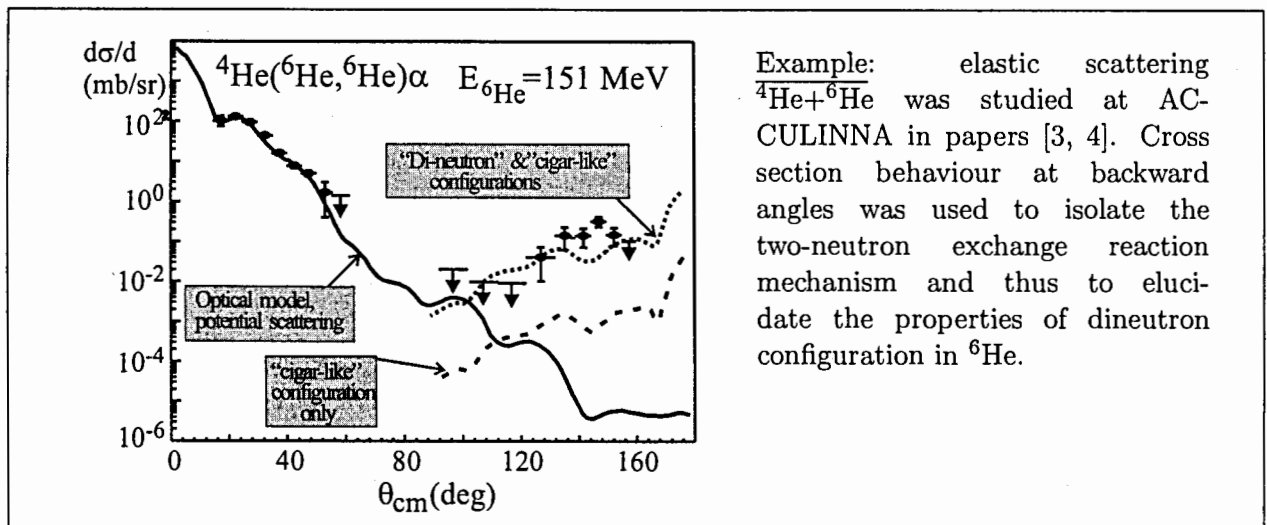
Example: To solve the ambiguity problem in establishing the ${}^6\text{He}+p$ and ${}^6\text{He}+A$ (where A is a nucleus with mass number A) optical potentials (OP’s) one should measure the differential elastic scattering and total elastic and reaction cross sections. This is important not only for obtaining the parameters of phenomenological OP’s themselves but mainly to search for the theoretically calculated microscopic OP’s. The characteristics of the microscopic ${}^6\text{He}+p$ OP’s are sensitive (a) to the density distribution of neutrons and protons of in ${}^6\text{He}$, and therefore this allows one to distinguish between different models destined for the description of the ${}^6\text{He}$ structure. Also, (b) the ${}^6\text{He}+A$ microscopic OP depends on the effective NN-forces in the overlapping region of colliding nuclei and thus can inform us on the incompressibility coefficient of nuclear matter in extreme conditions to compare this with the value obtained from the astrophysics data. Besides, (c) the energy dependence of the total reaction cross section and of the corresponding imaginary part of the ${}^6\text{He}+p$ OP at energies $E < 10$ MeV/amu is expected to be governed by the collective and decay properties of ${}^6\text{He}$ in its excited states rather than by its ground state structure.

The next frame shows another example of information which can be derived from the elastic

scattering experiments designated to the studies of clustering properties of exotic nuclei.

4.5 Inelastic scattering

This topic is an evident generalization of the previous one. It covers very broad range of reactions. We should only note here that (p, p') and (α, α') reactions provide straightforward way to access the excitation spectra of the exotic nuclei. The Coulomb dissociation, which we discuss below in details, is a special case of inelastic scattering. Contrary to this special case the general case of the inelastic scattering is defined by complicated interplay of nuclear and Coulomb interactions, which makes detailed interpretation of such data a complicated task.



4.6 Resonant elastic scattering

Among the resonant elastic scattering reactions the (p, p) and (α, α) reactions are of special interest. They are straightforwardly related to the radiative capture (p, γ) and (α, γ) reactions in nuclear astrophysics. The (α, α) reaction represents an effective tool for the study of α -cluster states in the spectra of nuclei⁵.

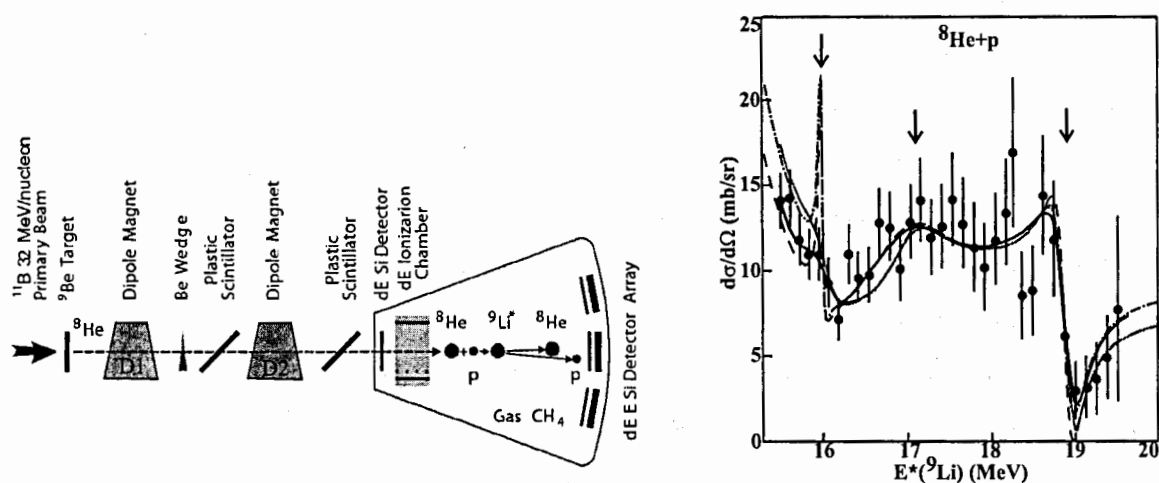
To work with exotic unstable nuclei these reactions should be performed in inverse kinematics. Nowadays a standard technique used in the resonant scattering experiments with RIBs is the Thick Target Inverse Kinematics (TTIK) method proposed by V.Z. Goldberg and co-workers [K.P. Artemov *et al.*, *Sov. J. Nucl. Phys.* **52** (1990) 408]. A development of the method using active targets was made (see e.g. Refs. [23, 35, 48]).

The TTIK method makes use of the large resonance scattering cross sections and small rate of energy loss typical for the light particles $(p, {}^4\text{He})$, as compared to the heavier projectile

⁵This topic is relevant to the very popular nowadays research of the Bose-Einstein condensation in nuclear systems.

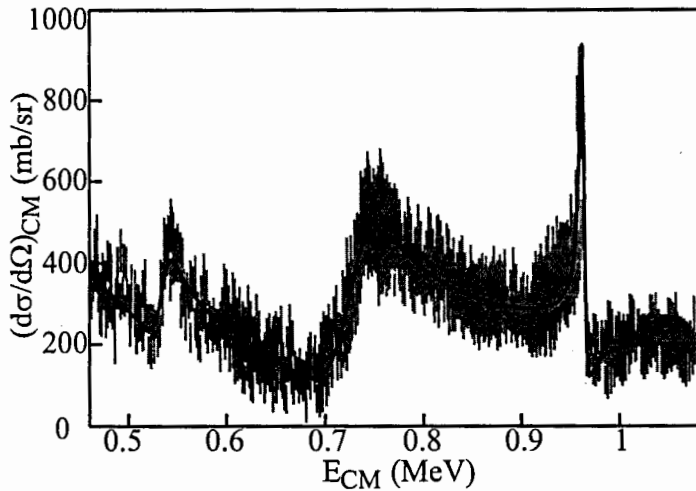
nuclei. Soon, it became evident that the TTIK method meets new demands made by the trend towards the study of resonance reactions induced by radioactive beams. These demands come from the nuclear astrophysics interest to understand the role of unstable nuclei in stellar processes (see, for example, [M. Wiescher *et al.*, *Ap. J.* **343** (1989) 352]), and from the interest to the physics of exotic nuclei. The typical binding energy of a nucleon in nuclei on the stability line is ~ 8 MeV. Therefore the excitation energies of the states which can be populated in the resonance scattering reactions are here above 8 MeV, i.e., accessible is only a region where the level density is high and the direct comparison with the theoretical predictions is difficult. The drip-line nuclei have low binding energies by definition. Therefore, the resonance scattering allows one to obtain the lowest excited states. It is also possible to study nuclei beyond the drip lines, starting from their ground states (see, for example, the case of ^{15}F [V.Z. Goldberg *et al.*, *Phys. Rev.* **C69** (2004) 024602]). Possibility to populate the lowest states of exotic nuclei means that the theory of exotic nuclear structure and the experiment can move hand-in-hand in these investigations. The new situation in nuclear physics which is connected to the current renaissance of resonance scattering can be demonstrated by the example of a $^8\text{He}+p$ resonance scattering experiment.

Example: proton resonance scattering was studied at ACCULINNA in the $^1\text{H}(^8\text{He},p)$ reaction in inverse kinematics [15]. In this experiment the properties of states in ^9Li with isospin $T = 5/2$, $T_3 = 3/2$, located above the $^8\text{He}+p$ threshold were obtained. The data obtained on these states can be easily related to the properties of the ground and the lowest excited states ($T = 5/2$, $T_3 = 5/2$) in the more neutron-rich system ^9He , due to the isobaric symmetry. The investigation of the high-lying isobaric analogue states with large T is an efficient way to infer definite knowledge on the properties of the lowest states in the neighbouring neutron-rich systems.



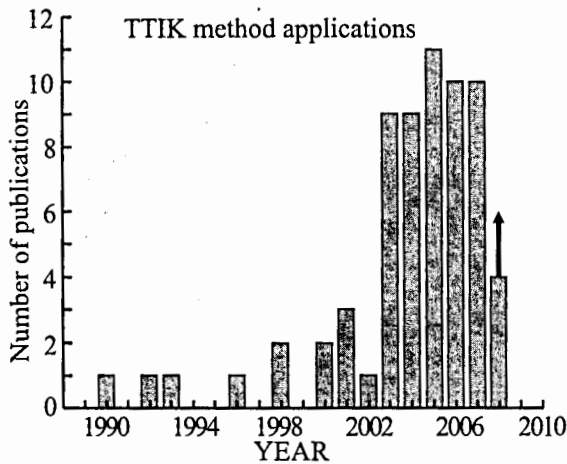
While experiments employing the TTIK method were done mostly using the beams of proton rich nuclei and (mainly solid, CH_2) proton targets, the data for the interactions of neutron-rich

nuclei with hydrogen and helium targets are scarce. Strong motivation for these studies comes from the interest to the study of very neutron-rich nuclei by means of their analogue states, as has been done in Ref. [15]. The corresponding experimental studies were restricted by the difficulties related to the operation of gas targets and due to the unclear role of the $T_{<}$ states. In this sense the work [15] made a breakthrough in the field. The special questions related to the application of the R-matrix analysis to the reactions induced by the exotic nuclei were also addressed in this work.



Example: the ^{16}F system is beyond the proton drip-line (all the states of ^{16}F belong to the $^{15}\text{O}+p$ continuum). The low-lying states of ^{16}F were investigated in the $^1\text{H}(^{15}\text{O},p)$ reaction at GANIL [I. Stefan *et al.*, arXiv:nucl-ex/0603020] having in mind astrophysical applications. Very precise information can be obtained in this class of reactions. The authors have found very precise values for the

energies and widths of different J^π states in ^{16}F : 0^- , $E = 534 \pm 5$ keV, $\Gamma = 25 \pm 5$ keV; 1^- , $E = 732 \pm 10$ keV, $\Gamma = 70 \pm 5$ keV; 2^- , $E = 958 \pm 2$ keV, $\Gamma = 6 \pm 3$ keV. It will be worth to note the recent paper by D.W. Lee *et al.* [Phys. Rev. C **76** (2007) 024314] where the authors reported a width of ~ 3 keV for a 947 keV level of ^{16}F .

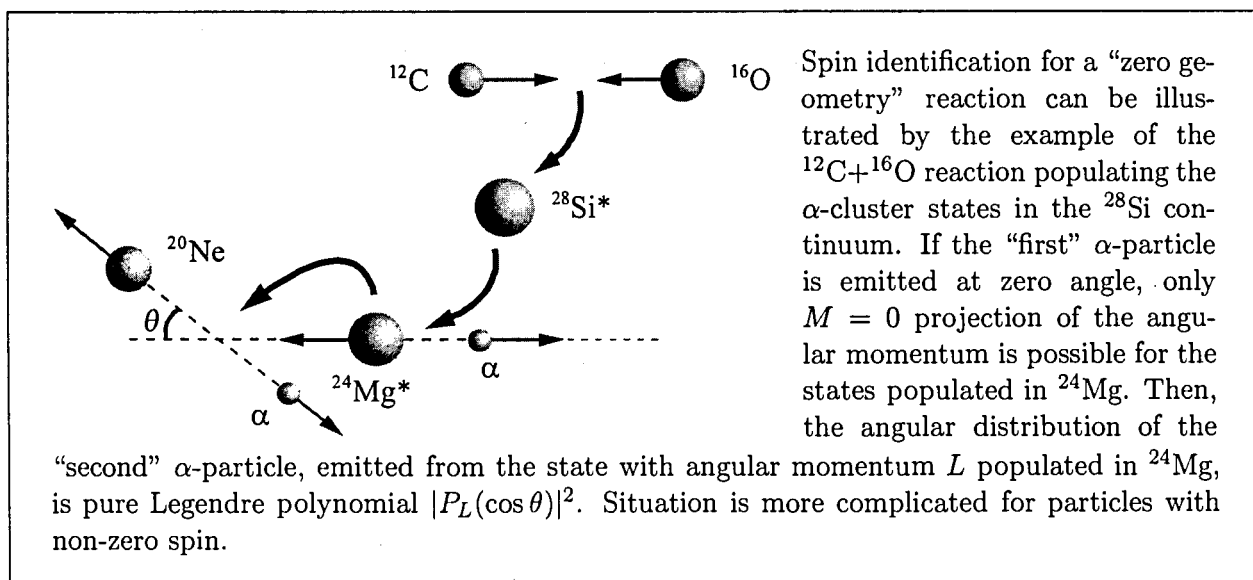


Surely, the study of the drip-line nuclei performed on the basis of the TTIK method will generate in future even more strong interest. This trend becomes evident from the diagram showing the number of papers published annually on the topic since 1990. We are planning to study the $^{20}\text{O}+p$ resonance interaction to obtain information on the ^{21}F structure, and the $^{14,15}\text{O}+\alpha$ interaction to study the resonances of astrophysical importance. The optimal energy of the radioactive beams for the investigations in question is in the region of 5 – 10 MeV/amu.

4.7 Transfer reactions

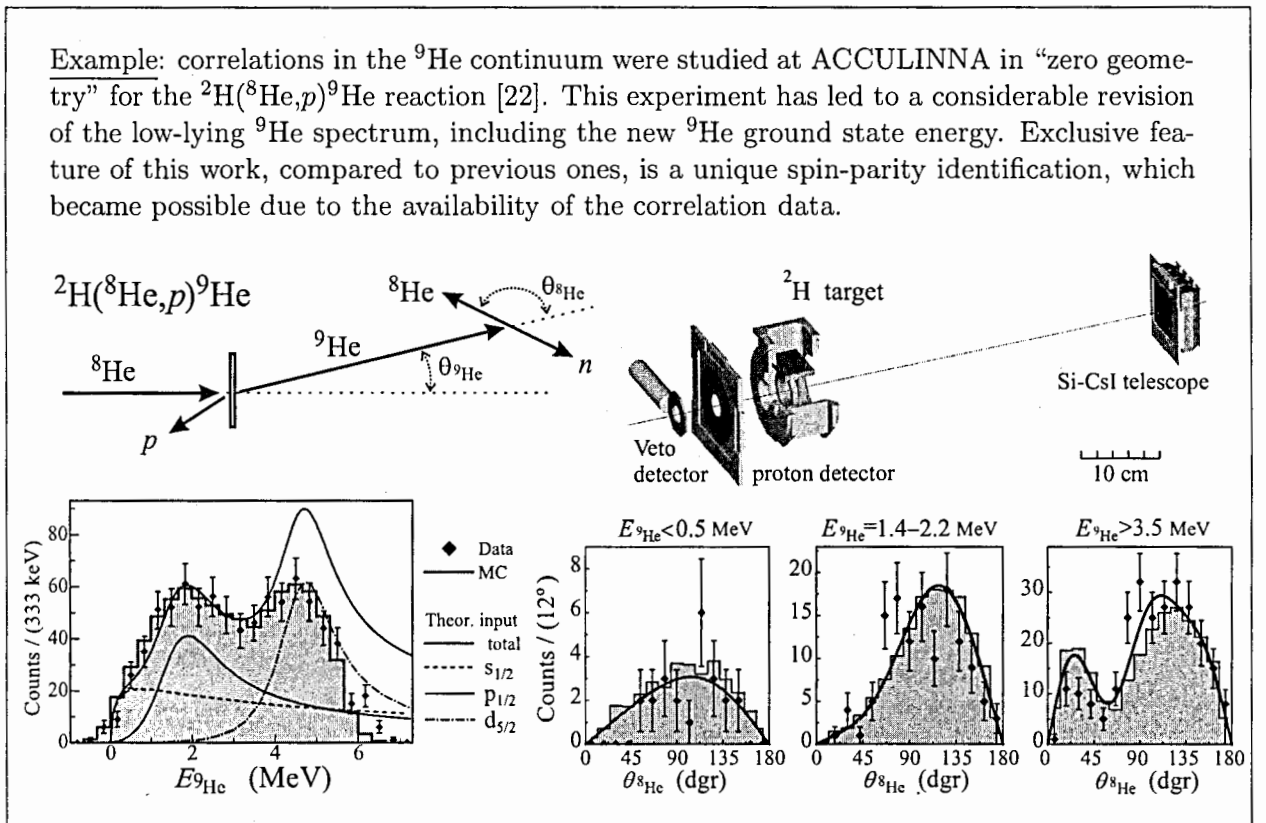
Nucleon/cluster transfer is an evident way to populate neutron/proton-rich systems in proximity and beyond the drip-lines. The cross sections of such reactions are relatively high — between a few millibarn and tens and hundreds of microbarn for one/two-nucleon transfer. At incident energy above 20 MeV/amu the one-step transfer dominates. The one-step transfer reactions are sufficiently well understood, they allow a reasonably simple theoretical treatment with a possibility to justify further simplifying assumptions⁶. There are clear methods to identify this reactions mechanism (e.g., the Goldberger-Treymann criterion). Maintaining the so called “zero geometry” for the one-step transfer reactions one obtains the population of highly spin-aligned states. This leads to the formation of expressed correlation patterns making possible unambiguous spin-parity identification.

To make a step away from the stability line using nuclei near the neutron drip-line one can employ either the neutron transfer to a neutron-excess exotic nucleus [the (d, p) , (t, p) reactions], or the proton removal reactions [e.g., the $(p, 2p)$, $(d, {}^3\text{He})$, $({}^3\text{H}, \alpha)$, $({}^6\text{Li}, 2\alpha)$ reactions]. Vice versa, one can investigate proton-excess nuclei either using the proton transfer [the (d, n) , $({}^3\text{He}, n)$ reactions] to proton-excess exotic nuclei, or the neutron removal reactions [(p, d) , (d, t) , (p, t) , $({}^3\text{He}, \alpha)$, $(\alpha, {}^6\text{He})$, $(\alpha, {}^8\text{He})$]. Evidently, the study of any of these reactions requires radioactive beams, which means that the inverse kinematics should be implemented with the target nuclei of hydrogen, helium or lithium isotopes. Lighter targets (the hydrogen isotopes and ${}^3\text{He}$) are preferable as they allow target-like recoils to leave the target and be registered. A number of (d, p) , (t, p) , $(p, 2p)$ reaction studies have been performed at ACCULINNA [8, 12, 14, 18, 20, 21, 22, 24, 25].



⁶These could be spin zero or dineutron transfer assumptions for the one-nucleon or two-neutron processes, respectively.

Experiments done at ACCULINNA with the use of the (d, p) and (t, p) reactions have shown a remarkable advantage of measurements performed for the small (e.g. $\sim 3 - 7^\circ$) centre-of-mass system (cms) angles. For ~ 30 MeV/amu RIB this corresponds to recoil protons emitted to reasonably large (e.g. $\sim 155 - 175^\circ$) backward angles in lab system making their detection quite easy and background free. On the other hand, the small reaction cms angles well correspond to the “zero geometry” condition, which practically guarantees that only the minimal magnetic sub-states are populated in the produced system. As it has been pointed previously this means maximal spin alignment and hence high probability for the observation of expressed correlation patterns. The existence of the expressed correlation patterns does not guarantee the unique spin-parity identification, but it can significantly facilitate such identification. Below the cases, where such identification was made for ^9He [22] and ^5H [20, 21] nuclei, are illuminated.

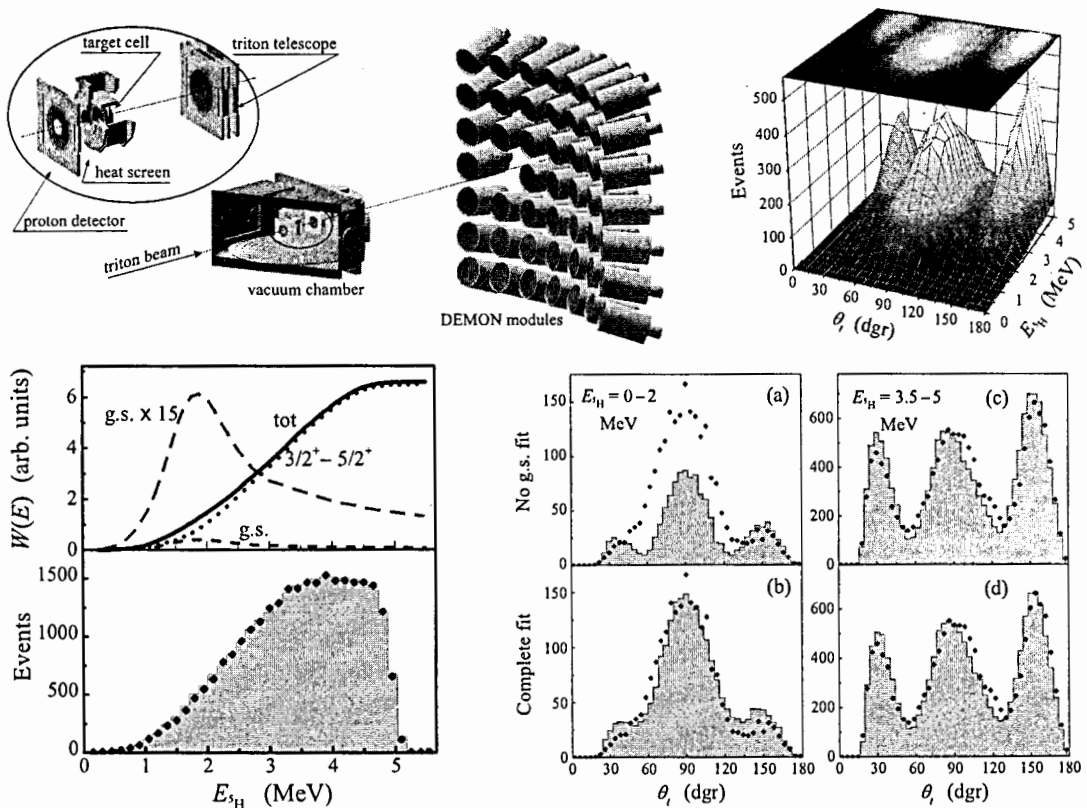


Distinctive feature of ACCULINNA is the accessibility of cryogenic tritium targets and triton beams. Such opportunities are not accessible elsewhere in the world. The tritium target provides access to a unique set of clean, background-free (t, p) reactions which bring us by two neutrons beyond the last accessible neutron-rich RIB. The (t, p) reactions can populate two-neutron continuum states in the neutron-rich nuclear systems. Though the study of such continuum states (mainly in the ^6He , ^8He , and ^{11}Li nuclei) was active in the recent years, the potential of this field as important source of information, remains poorly explored. Here, even the analysis and minimal interpretation of the measured data becomes a challenge and it requires

sophisticated theoretical tools. One example of such research performed at ACCULINNA (${}^5\text{H}$ case) is presented below.

Good energy resolution is highly desirable to resolve resonance states and provide reliable information on the energy spectra of exotic nuclear systems even in the cases where data are acquired with relatively small statistics. Special situation, where high invariant/missing mass resolution is indispensable, arises when virtual (*s*-wave) states become the subject of study. The problem of possible existence of virtual ground states in such systems as ${}^9\text{He}$, ${}^{10}\text{Li}$, ${}^{12}\text{Li}$ is under investigation for years without a great success. This is a problem relevant to the well known and long-standing theoretical problem of shell inversion occurring at the neutron drip-line (the $2s_{1/2}$ state goes below $1p_{1/2}$ in certain theoretical scenarios).

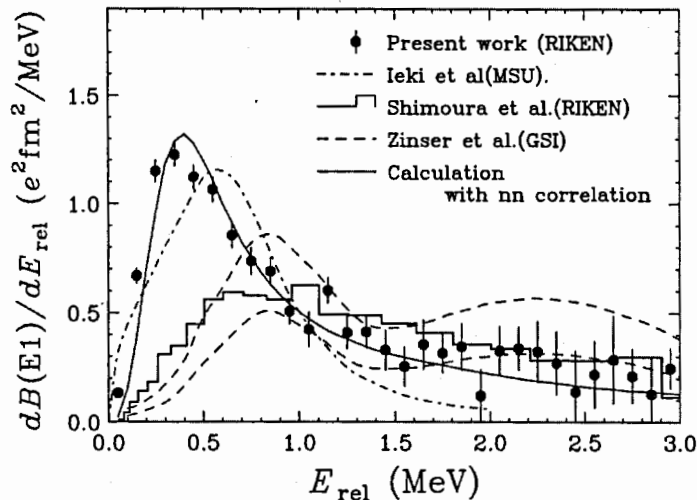
Example: Correlations in the ${}^5\text{H}$ continuum were studied at ACCULINNA in “zero geometry” conditions realized for the ${}^3\text{H}(t,p){}^5\text{H}$ reaction [20, 21]. The three-body correlation patterns observed in this experiment allowed us to disentangle a small contribution of the $1/2^+$ ground state from the thick “background” originating from the low-energy wing of the $3/2^+-5/2^+$ doublet of the ${}^5\text{H}$ excited states. Special theoretical methods suitable for the analysis of the three-body decays of spin-aligned systems were developed to make this analysis possible.



4.8 Coulomb dissociation

Coulomb dissociation is, evidently, a special case of inelastic excitation. Electromagnetic dissociation is one of the best methods to study excitation spectra of drip-line nuclei. Its nature is well established and theoretical methods have been developed allowing quantitative interpretation of the data. A well known approach to be mentioned here is the semiclassical theory of Alder and Winter treating in a time-independent way the interaction of colliding nuclei. In this approach dissociation occurs due to the absorption of “virtual photons” generated by the motion of the projectile in the variable electromagnetic field of the heavy target along the classical Coulomb trajectory. This makes the electromagnetic dissociation formally analogous to the photo dissociation. Contrary to the “genuine” nuclear reactions, the availability of reliable theoretical tools reduces considerably the uncertainty of the information deduced from the experimental results on the electromagnetic dissociation.

For the Coulomb dissociation reactions the highest possible incident beam energies are preferable: this provides hard and intense spectrum of virtual photons enabling large dissociation probability into a broad final-state energy range. The low-energy case is more challenging from theoretical point of view and requires more theoretical contribution for reliable interpretation of the data. However, problems arising here are known to be tractable. A successful list of relatively low energy studies exists for the drip-line nuclei (e.g., at energies ~ 50 MeV/amu and below).



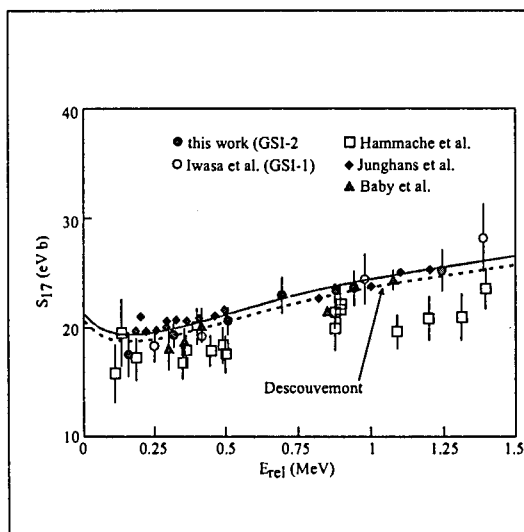
730], GSI [M. Zinser *et al.*, Nucl. Phys. **A619** (1997) 151] and old RIKEN data [S. Shimoura *et al.*, Phys. Lett. **B348** (1995) 29] are not in mutual agreement. This situation evidently requires further studies.

Example: For the two-fragment dissociation reactions ($^{11}\text{Be} \rightarrow ^{10}\text{Be} + n$, $^8\text{B} \rightarrow ^7\text{Be} + p$) almost all experiments give similar results. However, for the three fragment dissociation ($^6\text{He} \rightarrow ^4\text{He} + n + n$, $^{11}\text{Li} \rightarrow ^9\text{Li} + n + n$) the reported experimental data are contradictory. Figure from paper [T. Nakamura *et al.*, Phys. Rev. Lett. **96** (2006) 252502] illustrates this situation. The data from MSU [K. Ieki *et al.*, Phys. Rev. Lett. **70** (1993)

Low binding energies and appearance of the halo phenomenon is common situation close to the drip-line. Based on the halo hypothesis the existence of a novel dipole mode at low excitation

energies has been suggested in the late eighties [K. Ikeda, INS report JHP-7, 1988, in Japanese] and later was found experimentally. This so-called soft mode of giant dipole resonance is related to the low binding energy of the halo neutrons which allows low-frequency oscillations of the halo neutrons against the core creating the low-lying dipole excitations. The soft dipole mode is characterized by strong concentration of the E1 strength near the dissociation threshold in halo nuclei and, hence, large electromagnetic dissociation cross sections. Nowadays, the soft dipole mode phenomenon seems to be quite common for the drip-line nuclei (it has been established in ${}^6\text{He}$, ${}^8\text{He}$, ${}^{11}\text{Li}$, ${}^{11}\text{Be}$, ${}^8\text{B}$, and is the subject of investigation in the two-proton halo nucleus ${}^{17}\text{Ne}$). In the heavier drip-line nuclei (e.g., in ${}^{22}\text{O}$, ${}^{132}\text{Sn}$, etc.) it arises in the form of the so-called “pygmy” dipole resonance.

Coulomb dissociation cross sections are straightforwardly related to the probability of the astrophysical non-resonant radiative capture (the Coulomb dissociation can be interpreted as a reverse process). This justifies great efforts concentrated on this topic over the past decade and, in particular, on the breakup of ${}^8\text{B}$. In Coulomb dissociation the low-energy part of the excitation spectrum is amplified by the low-energy rise of the virtual photon spectra. This is a serious advantage of the Coulomb dissociation studies in nuclear astrophysics compared to direct elastic cross section measurements. Such reactions as the three-body radiative capture ($2p$ capture, $2n$ capture, triple- α reaction) can not be directly studied in laboratory at all. Opportunities provided by Coulomb dissociation are unique for this class of reactions.



Example: results of Coulomb dissociation studies of the famous S_{17} astrophysical factor [F. Schümann *et al.*, Phys. Rev. C **73** (2006) 015806] and [N. Iwasa *et al.*, Phys. Rev. Lett. **83** (1999) 2910]. The S_{17} value defines the intensity of the radiative capture reaction ${}^7\text{Be}(p, \gamma){}^8\text{B}$ at the energies of astrophysical interest (Gamow peak energy for this reaction is at about 20 keV for the Sun core). Direct measurements of this reaction are very complicated (the data are from [F. Hammache *et al.*, Phys. Rev. Lett. **86** (2001) 3985], [L.T. Baby *et al.*, Phys. Rev. Lett. **90** (2003) 022501], and [A.R. Junghans *et al.*, Phys. Rev. C **68** (2003) 065803]).

4.9 Knockout reactions and quasi-free scattering

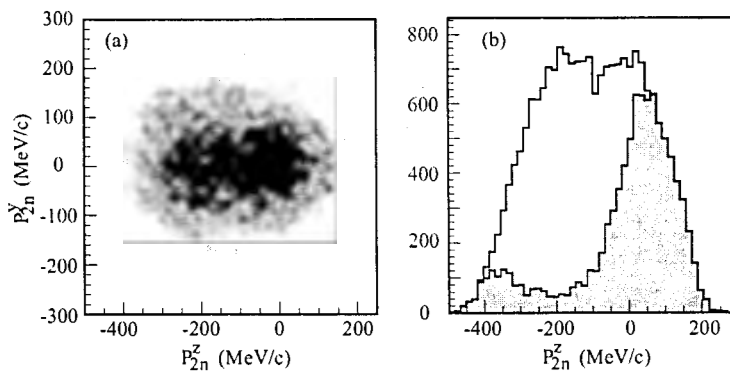
These reactions represent a significant part of the research at in-flight RIB facilities. They have large cross sections and allow simple theoretical interpretation (within such approaches as, e.g., the Plane Wave Impulse Approximation, PWIA). These reactions are widely used for the

experimental study of nuclear structure: they provide an access to single-particle and cluster degrees of freedom.

Light exotic nuclei near the drip-lines are very suitable objects for the study of their structure by means of quasi-free reactions. Appropriate experiments involving the so-called Borromean nuclei, ${}^6\text{He}$, ${}^{11}\text{Li}$, ${}^{17}\text{Ne}$, could provide data on exotic correlations predicted by theory for these nuclei. The knockout of strongly bound protons and clusters from the nuclei in the vicinity of the neutron drip-line can provide an access to the extremely neutron-rich nuclear systems beyond the drip-line with the N/Z ratio more than 5. The neutron shell structures are assumed to be similar in the sequences of hydrogen ${}^{5,6,7}\text{H}$ and helium ${}^{6,7,8}\text{He}$ isotopes, so one could expect the production of super-heavy hydrogen isotopes in the reactions like ${}^1\text{H}({}^6\text{He}, 2p){}^5\text{H}$, ${}^1\text{H}({}^8\text{He}, pt){}^5\text{H}$, ${}^1\text{H}({}^8\text{He}, pd){}^6\text{H}$, ${}^1\text{H}({}^8\text{He}, 2p){}^7\text{H}$. The α knockout reactions from ${}^{14}\text{Be}$, like ${}^4\text{He}({}^{14}\text{Be}, 2\alpha){}^{10}\text{He}$, ${}^4\text{He}({}^{14}\text{Be}, \alpha^3\text{He}){}^{11}\text{He}$ could be perspective for the study of the ${}^{10,11}\text{He}$ systems.

A test case to the concept supposing the use of quasi-free scattering at a RIB energy typical to ACCULINNA could be the ${}^4\text{He}({}^6\text{He}, 2\alpha)2n$ and ${}^4\text{He}({}^8\text{He}, 2\alpha)4n$ reactions. The following example gives some notion about the perspectives of this kind of research.

Example: The quasi-free scattering reaction ${}^4\text{He}({}^6\text{He}, 2\alpha)2n$ was studied at ACCULINNA using a 25 MeV/amu ${}^6\text{He}$ beam [46, 47]. The left panel shows the distribution of the observed events in the P_{2n}^y vs. P_{2n}^z plot, where P_{2n}^z and P_{2n}^y are, respectively, longitudinal and transverse components of the $2n$ cms momentum. Those events which gather around the $P_{2n}^z = 0$ point correspond to the quasi-free $\alpha - \alpha$ scattering (the neutron pair is a spectator). One can see a reasonable separation between the locus of the quasi-free events and another group of events tending to $P_{2n}^z \sim -200$ MeV/c. This group corresponds to the neutron pairs emitted in competing reactions from a system moving together with the ${}^6\text{He} + {}^4\text{He}$ cms. The distribution of the longitudinal momentum component is shown in the right panel for the bulk of the data and for events satisfying condition $E_{\alpha-2n} > 20$ MeV. At this condition the contribution of competing reactions is suppressed and the bump in the vicinity of $P_{2n}^z = 0$ corresponding to the quasi-free scattering is clearly seen. The novel feature of such kind of “core knock-out” experiments is that they provide access to the momentum distribution of



the two-neutron subsystem in the halo nucleus. So far, for the two-neutron halo nuclei the properties of the halo neutron subsystems were typically investigated in the nucleon-removal reactions.

Characteristics obtained in the discussed reactions are the momentum distributions of the “residual” fragments. For the one-nucleon halo this information is typically sufficient to deduce information about the shell composition (s , p , d , etc.). The following example illuminates this point.

Example: The knockout reaction ${}^9\text{Be}({}^{11}\text{Be}, {}^{10}\text{Be}+\gamma)$ at 60 MeV/amu has been used to determine the ground state structure of ${}^{11}\text{Be}$ [T. Aumann *et al.*, Phys. Rev. Lett. **84** (2000) 35]. The obtained data allowed an accurate determination of the longitudinal momentum distribution for the removal of a $1s$ neutron leading to the ${}^{10}\text{Be}$ ground state. The distribution agrees reasonably well with calculations and confirms the validity of the knockout models for extracting structure information. The partial cross sections for the four lowest excited ${}^{10}\text{Be}$ states are in good agreement with calculations based on the shell model and the eikonal reaction theory. The results provided the support to a picture in which the ${}^{11}\text{Be}$ ground state is dominated by the $1s$ single-particle component with a small $d_{5/2} \otimes 2^+$ admixture.

Knockout reactions are well established as a spectroscopic tool. Accompanied by γ -spectroscopy these reactions can provide an access to the single-particle structure of a fragmented system. The preceding example is a good illustration of this point: the conclusion made about the domination of the $1s$ single-particle component in the ${}^{11}\text{Be}$ ground state is based on the selection of events in coincidence with γ -rays emitted by the ${}^{10}\text{Be}$ fragments.

For the two-nucleon Borromean systems both the momentum distributions of individual fragments and distributions of the residual unbound system can be obtained. The example presented below shows the prospects of this approach for the study of energy spectra of the extremely neutron-rich nuclear systems.

Example: Fragmentation processes have been studied with ${}^{11}\text{Li}$ (264 MeV/amu) and ${}^{14}\text{Be}$ (287 MeV/amu) beams bombarding carbon target [H. Simon *et al.*, Nucl. Phys. **A791** (2007) 267]. Experimental conditions enabled the authors to separate the neutron knockout channels. The one-neutron knockout made it possible to determine the properties of the unstable ${}^{10}\text{Li}$ and ${}^{13}\text{Be}$ intermediate systems. The observed fragment-neutron angular correlations exhibit asymmetry. The authors consider this to be a fingerprint of contributions from states with different parities (s -, p - and d -waves). The presence of such configurations is confirmed by the analysis of the fragment momentum distributions. In the case of ${}^{10}\text{Li}$, a p -state was observed at 0.51(4) MeV and there was an evidence for a d -state at 1.49(9) MeV. The low-energy part of the ${}^9\text{Li} + n$ energy spectrum is dominated by an s -wave virtual state with a scattering length of about ~ -30 fm. The authors arrived at a conclusion that the s -wave interaction between the neutron and ${}^{12}\text{Be}$ fragment is much weaker than that in the ${}^9\text{Li} + n$ case. The $J^\pi = 1/2^-$ assignment to the ${}^{13}\text{Be}$ state at 3.04(7) MeV was made from comparison with the neighbouring $N = 9$ isotones, and was additionally confirmed by the measured ${}^{12}\text{Be}$ - n angular correlations.

4.10 Radioactive decays

Radioactive decays of the nuclei around the drip-line are typically investigated in two ways.

4.10.1 Beta-delayed decays

Nucleon-stable systems located quite far from the “ β -stability valley” have large Q_β values. As a result, probability for the β -decays to proceed to the states above the particle (cluster) emission thresholds in the daughter systems becomes considerable. This leads to enhanced probability of the β -delayed particle emission. Considerable efforts were invested in the studies of such radioactive decays in the lightest exotic nuclei: ${}^6\text{He} \rightarrow \alpha + d$, ${}^8\text{He} \rightarrow \{{}^7\text{Li} + n, \alpha + t + n\}$, ${}^9\text{Li} \rightarrow \alpha + \alpha + n$, etc. Still, even this particular field is far from complete clarity. If we turn to the s - d shell and to the heavier nuclei, the knowledge about the β -delayed particle (cluster) emission branchings appears to be quite fragmentary. A curious demonstration of this fact is the recent discovery of the *three-proton* β -delayed branch of the ${}^{45}\text{Fe}$ decay [K. Miernik *et al.*, Phys. Rev. C **76** (2007) 041304(R)].

The β -delayed decay represents an evident way to get access to the properties of the continuum excitation spectra of exotic nuclei in a broad energy range⁷ and it evidently has a direct relation to the astrophysical burning cycles (the particle emission branch returns the process back in the course of the nucleosynthesis).

It is interesting to note that the β -delayed proton decay was for the first time identified at FLNR [V.A. Karnaukhov *et al.*, JETPh, **45** (1963) 1280].

4.10.2 Particle or cluster radioactivity

Beyond the driplines the ground state particle (cluster) radioactivity may become possible. In heavy nuclei, the ground state α -decays are common; the Gamow theory of α -radioactivity is among the most important milestones leading to the establishment of quantum mechanics. The issue of proton radioactivity has been discussed since 1948. In 1970 the proton radioactivity was discovered by the example of the isomer of ${}^{53m}\text{Co}$ [J. Cerny *et al.*, Phys. Lett. **33B** (1970) 284] and in 1982 the ground-state radioactivity was for the first time found in ${}^{151}\text{Lu}$ [S. Hofmann *et al.*, Z. Phys. **A305** (1982) 111]. In 1960 the possibility of the two-proton ground state radioactivity was predicted for a broad range of drip-line nuclei in the classical paper of Goldansky [V.I. Goldansky, Nucl. Phys. **19** (1960) 482].

One can expect the ground state proton radioactivity decays for $Z > 50$ nuclei which are out of the reach of the proposed facility. In lighter proton-rich systems beyond the drip-line we

⁷This is restricted, of course, by the energy window accessible in the Q_β decay and by the selectivity of this process.

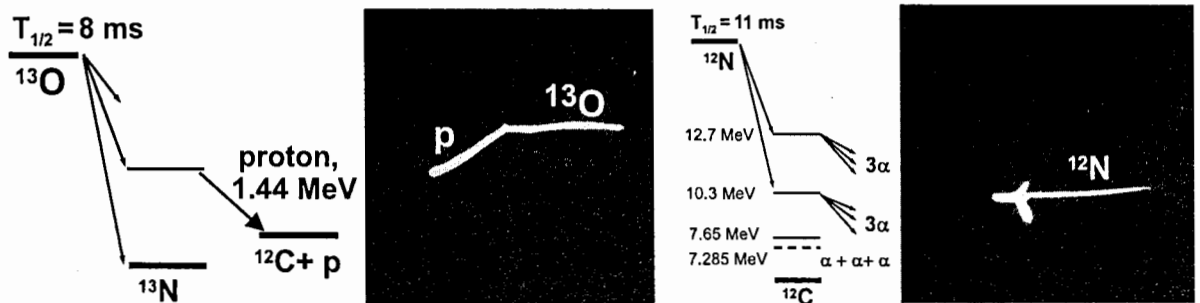
should speak rather about the proton unstable ground state resonances (which are too broad to be considered in terms of radioactivity). The two-proton radioactive decays, however, could take place in the much lighter systems. Contrary to the proton radioactivity which is under scrutiny for decades, the two-proton radioactivity has been discovered in ^{45}Fe only few years ago [M. Pfützner *et al.*, *Eur. Phys. J. A* **14** (2002) 279; J. Giovinazzo *et al.*, *Phys. Rev. Lett.* **89** (2002) 102501]. This is now a very hot topic in nuclear physics and it attracts a lot of attention, both from the experimental and theoretical sides. Very recently the ground state two-proton radioactivity was found at GSI for the lightest possible case — the ^{19}Mg isotope [I. Mukha *et al.*, *Phys. Rev. Lett.*, **99** (2007) 182501].

The two-proton radioactivity remains still unexploited phenomenon in the drip-line nuclei from ^{19}Mg to ^{45}Fe . This provides a broad field for the investigation at the proposed facility. As it has already been mentioned, the (d, n) and $(^3\text{He}, n)$ reactions of proton-rich RIBs constitute a suitable way to produce nuclei lying beyond the proton drip-line.

4.10.3 Novel experimental methods

Wide-spread approach to the radioactive decay study makes use of the implantation technique: the mother nucleus is implanted in a solid-state detector and the decay energy signal is measured. Recently, other, more powerful methods become available in the study of rare decay events. Among these methods the time projection chambers are notable. In particular, one should mention the optical time projection chamber (OTPC) [48]. In this device the RIB nuclei are stopped in the chamber volume and the drift of the charge carriers created in gas is conver-

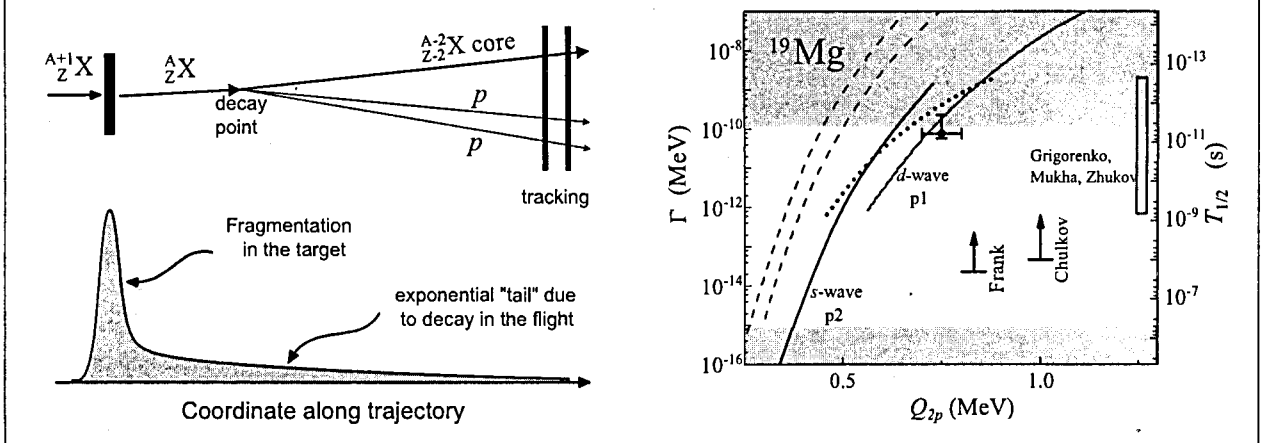
Example: Recently a very bright result was obtained at MSU: the two-proton correlations from the ground state two-proton radioactive decay of ^{45}Fe were measured by OTPC technique [K. Miernik *et al.*, *Phys. Rev. Lett.*, **99** (2007) 192501]. An essential preparation stage to this experiment was the test irradiations done at ACCULINNA where the β -delayed proton and α decays of several nuclei were used to tune the OTPC systems [48]. The OTPC images of the decay events from the ACCULINNA experiment shown below illustrate the device performance. The β -delayed particle emission off ^{13}O (into $^{12}\text{C}+p$ continuum) and ^{12}N (into $\alpha+\alpha+\alpha$ continuum) are shown.



ted in light processed by a special CCD camera. Combined with the measured drift time the obtained image allows one to have a complete kinematics reconstruction of the events with efficiency close to unity. The later is very important for the rare decays of exotic species.

Another novel approach to the radioactivity studies employs tracking technologies taken from the plunger technique developed in 70th for the study of shape isomers [V. Metag, *et al.*, Nucl. Instr. Meth. **114** (1974) 445; G. Ulfert, *et al.*, Nucl. Instr. Meth. **148** (1978) 369] and high-energy physics. The implantation technique has a natural limitation from the time required for RIB separation. The lifetimes shorter than a few milliseconds, for the ISOL method, and hundreds of nanoseconds, for the in-flight separation, cannot be measured by the implantation technique. In the decay-in-flight method the shortest measurable lifetimes are some picoseconds. The flight distance is defined by precision tracking of the decay products. This method drastically (by four orders of the magnitude) increases the range of lifetimes accessible for experimental investigation.

Example: The two-proton decays of several *s-d* shell nuclei were studied recently at GSI by means of the decay-in-flight method [I. Mukha *et al.*, Phys. Rev. Lett., **99** (2007) 182501]. These experiments employed an advanced micro-strip detector array. The ^{19}Mg isotope was discovered, and correlations were studied for the two-proton decay of its ground state. The lifetime of ^{19}Mg , found to be 4.6(15) ps, is the shortest radioactive decay lifetime ever measured. The basic idea of the experiment is illustrated in the left panel. In the right panel the measured value is compared with theoretical predictions [L.V. Grigorenko *et al.*, Nucl. Phys. **A713** (2003) 372]. The gray hatching shows the boundaries of the decay-in-flight method: for the small lifetimes the track is too short to be measured, for the large lifetimes the implantation technique becomes possible.



4.11 Breakup reactions in general and continuum spectroscopy

One can single out a class of experiments where the main interest is to get access to the properties of the continuum excited states of the exotic projectile nucleus which are populated at its breakup. The breakup specific reaction, and its behaviour, may be the subject of interest to

the extent of how the excitation spectrum population depends on this. The Coulomb dissociation reactions and, e.g., transfer reactions populating continuum states could be also regarded as the representatives of this broader class of the processes capable to elucidate the continuum excitation properties. Breakup processes on the light targets, characterized by the strong Coulomb-nuclear interference and diffractive dissociation, are an alternative to the Coulomb dissociation breakup reactions. They could have different selectivity in quantum numbers compared, say, to the Coulomb dissociation which almost exclusively populates the E1 and E2 states. The most interesting possibility here is to study the breakup reactions in complete kinematics for the breakup products.

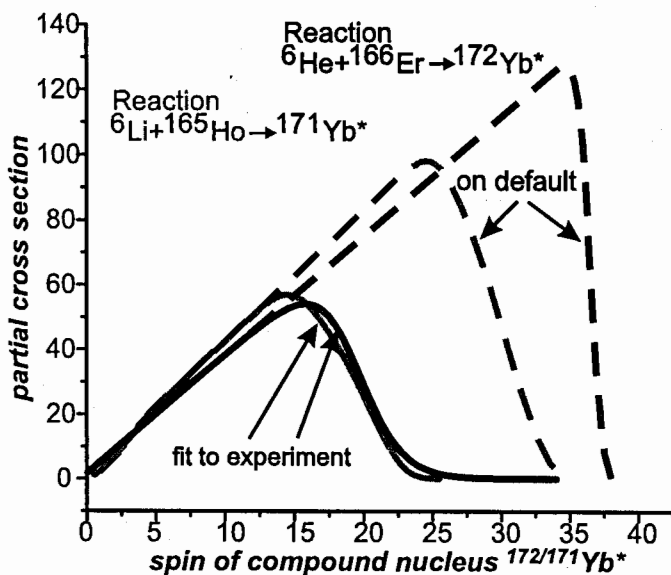
Correlations observed for the decay products originating from the continuum spectra carry information about the final state interactions. By ascertaining relevant correlation functions one could approach to the estimates of the emission region sizes [the so-called intensity interferometry or HanburyBrown-Twiss (HBT) interferometry]. Despite the fact that the three-body correlations were demonstrated to be an efficient tool for the spectroscopy of the Borromean systems, the potential of such correlations studies still remains poorly exploited. A good example here is the actively discussed possibility of the existence of the three-body virtual states. The ground states of ^{10}He and ^{13}Li could be such three-body virtual states. Just as it occurs with the ordinary two-body virtual states, these objects rather resemble the final state interactions than they are the real states characterized by a compact size and a definite lifetime. From theoretical point of view, the three-body virtual states appear to be a phenomenon closely related to the so-called Efimov effect recently discovered in atomic physics.

4.12 Fusion-evaporation and incomplete fusion reactions

Interplay between the fusion-evaporation and incomplete fusion reactions attracted much attention with particular emphasis put to the low-energy collisions of the halo nuclei with the medium mass and heavy targets. Numerous experimental results and theory considerations are summarized in the review papers by J.F. Liang and C. Signorini [J. Mod. Phys. **E14** (2005) 1121], L.F. Canto *et al.* [Phys. Rep. **424** (2006) 1], and by N. Keeley, *et al.* [Prog. Part. Nucl. Phys. **59** (2007) 579]. At relatively high energies with respect to the Coulomb barrier different processes can take place, in general, in the nucleus-nucleus collisions. In the case of the loosely bound RIB nuclei, the complete fusion cross section appears to be diminished due to the increased role of direct processes [A. Navin *et al.*, Phys. Rev. C **70** (2004) 044601]. Hence, it would be desirable to get data on the partial wave contributions into the different reaction mechanisms occurring with the loosely bound nuclei. At the beam energies well above the barrier the use of such semiclassical approximation is customary.

In the same experiment a number of reaction products originating from incomplete fusion were detected in coincidence with outgoing fragments resulting from the projectile breakup. For such evaporation residues one can analyse the measured populations of excited states with different spin values. This can allow to extract information on the excitation energy and angular momentum distributions of the initial compound nuclei that arise as a result of the incomplete fusion processes. This information is closely related to the mechanism of the breakup and incomplete fusion process and the wave function of the loosely bound projectile nucleus. In addition, in the same experiment one can obtain the pattern of excited states populated in the heavy target nuclei as a result of inelastic scattering reactions. These data can give access to the knowledge about the excitation spectrum occurring in the case of the projectile breakup.

Example: Complete fusion (CF) and breakup reactions initiated by ${}^6\text{He}$ halo nuclei were investigated recently in the interaction with medium mass target ${}^{166}\text{Er}$ at a ${}^6\text{He}$ beam energy $E_{\text{lab}} = 55 - 64$ MeV. The ${}^6\text{Li}+{}^{165}\text{Ho}$ and ${}^6\text{Li}+{}^{166}\text{Er}$ reactions were studied for comparison at a projectile energy 58 MeV [S.A. Krupko *et al.*, Book of Abstr. FUSION08 Sept. 21-26 2008, Chicago, USA, p. 50]. The experiments were performed using the DRIBs facility and a detector system based on six HP Ge detectors with BGO shells, a charged particle telescope and an array of neutron detectors consisting of eight units of the time-of-flight spectrometer DEMON. Population probabilities were measured for the levels of the ground-state rotational band and for band-8 in ${}^{166}\text{Yb}$. The critical values of the orbital momentum, l_{crit} , and diffuseness parameter D_l characterizing the width of the orbital momentum region where the transmission coefficients T_l change to zero from the unit value inherent to the small l partial waves were deduced from the data analysis done with the use of code EMPIRE [M. Herman *et al.*, Nucl. Data Sheets, 108 (2007) 2655]. Results obtained for the CF reactions ${}^{166}\text{Er}({}^6\text{He}, 6n){}^{166}\text{Yb}$ and ${}^{165}\text{Ho}({}^6\text{Li}, 5n){}^{166}\text{Yb}$ are shown in Figure. The best fits to the data

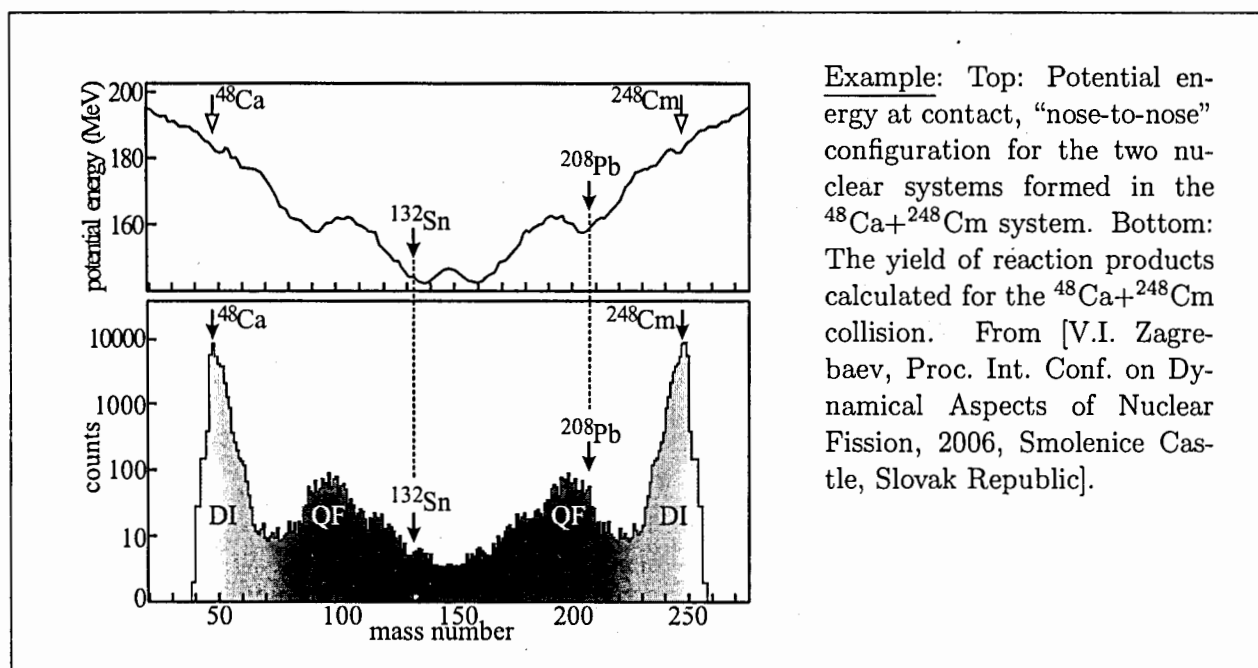


were obtained with $l_{\text{crit}} = 19.3$ and 18.6, respectively, for the reactions induced by ${}^6\text{He}$ and ${}^6\text{Li}$. A difference between the ${}^6\text{He}$ and ${}^6\text{Li}$ projectiles from the point of view of the fusion probability is foreseen. The broad gaps are obtained in the high angular momentum regions where complete fusion does not take place. A reasonable assumption is that in these regions incomplete fusion and/or breakup become the main reaction channels especially for the ${}^6\text{He}$ case.

Many drip-line nuclei accessible from ACCULINNA-2 as RIB projectiles with energy 10–50 MeV/amu can be the subject of studies performed in the way outlined here.

4.13 Study of the quasi-fission reaction using in-flight separation

Deep inelastic (DI) scattering and quasi-fission (QF) may dominate at incident energies around the Coulomb barrier in situation where the complete fusion probability could be rather small. To make clear this point an example of the potential energy surfaces for the $^{48}\text{Ca}+^{248}\text{Cm}$ nuclear system is shown below. The QF processes are not only determined by a simple diffusion process but also by the shell structure of the nuclear system. The latter can be seen in the bottom panel as a rather enhanced yield obtained for the fragments in vicinity of the doubly magic ^{208}Pb . However, due to lack of experimental methods, precise measurements with an unambiguous (A, Z) identification of quasi-fission fragments have never been done. Our interest is the light peak of the quasi-fission products, conjugated to the ^{208}Pb group. Being in-flight separated, these light QF fragments could be obtained as very neutron-excess RIB projectiles. In that case, it becomes more preferable for the $^{48}\text{Ca}+^{238}\text{U}$ system to have the light quasi-fission peak (^{78}Zn) closer to the neutron drip-line.



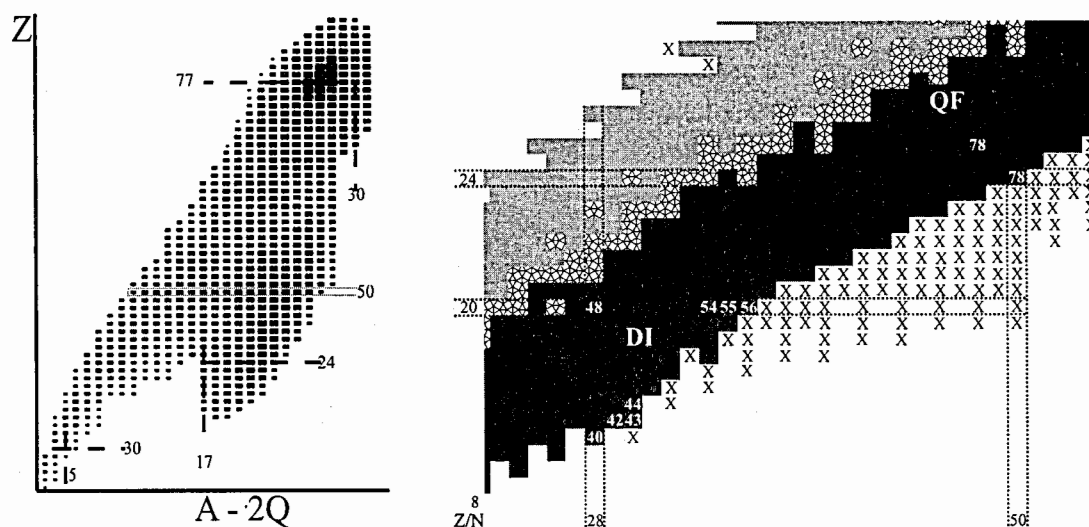
Example: Top: Potential energy at contact, “nose-to-nose” configuration for the two nuclear systems formed in the $^{48}\text{Ca}+^{248}\text{Cm}$ system. Bottom: The yield of reaction products calculated for the $^{48}\text{Ca}+^{248}\text{Cm}$ collision. From [V.I. Zagrebaev, Proc. Int. Conf. on Dynamical Aspects of Nuclear Fission, 2006, Smolenice Castle, Slovak Republic].

We propose to explore neutron-rich isotopes around ^{78}Zn using in-flight separation technique to identify unambiguously quasi-fission fragments. This will allow, for the first time, to identify individual QF fragments and to measure their production cross sections and energy spectra. The transmission provided by ACCULINNA-2 for such QF fragments will be higher by one order magnitude as compared to ACCULINNA. Another important advantage of ACCULINNA-2 will be excellent cleaning factor achieved for these RIBs due to the use of RF-filter.

The most difficult aspects of these studies come from the energy losses and mixing of different charge states of the primary beam and the QF fragments. It becomes difficult to achieve

sufficient detector resolution to identify the products. Keeping in mind this aspect of the work, one could firstly identify the known isomers (e.g., $^{67-70}\text{Ni}$, ^{78}Zn , ^{74}Ga) having lifetimes in the microsecond region. Fragments in the region of interest can be identified by measuring their time of flight (TOF), energy loss (Δ), kinetic energy, horizontal position in the dispersive plane (DPX). The DPX value is used to calculate effective $B\rho$ for each particle. The second example presented here shows Z vs. $(A - 2Q)$ plot reconstructed from the data taken at the NSCL [O.B. Tarasov. MSU experiment 5120. Private communication].

Example: Left panel shows the identification plot [O.B. Tarasov. MSU experiment 5120. Private communication] of projectile fragmentation and abrasion-fission fragments produced with a 80 MeV/amu ^{208}Pb beam and separated by the A1900 fragment-separator. Right panel shows the section of the chart of nuclei demonstrating the locations of the light quasi-fission and deep inelastic products. Particle bound nuclei are shown by crosses according to the prediction of the TYUU model [Atomic. Data Nucl. Data Tables, **39** (1988) 185; edited by P.E. Haustein].



Intensity estimates for the production rates of the RIBs of the quasi-fission fragments were done by means of code LISE++ [O.B. Tarasov, D. Bazin, Nucl. Phys. **A746** (2004) 411; <http://www.nsl.mscl.msu.edu/lise>]. The calculations assumed a two-body model for the reaction kinematics and a 1 mb cross section for the yield of the light fragments. These estimates show that within a one-hour experiment one could rely on the observation of more than ten new, unknown neutron-rich nuclei in the region of $Z = 25 - 30$. This shows that the quasi-fission reactions could be suitable for the production of intense low-energy neutron-rich RIBs.

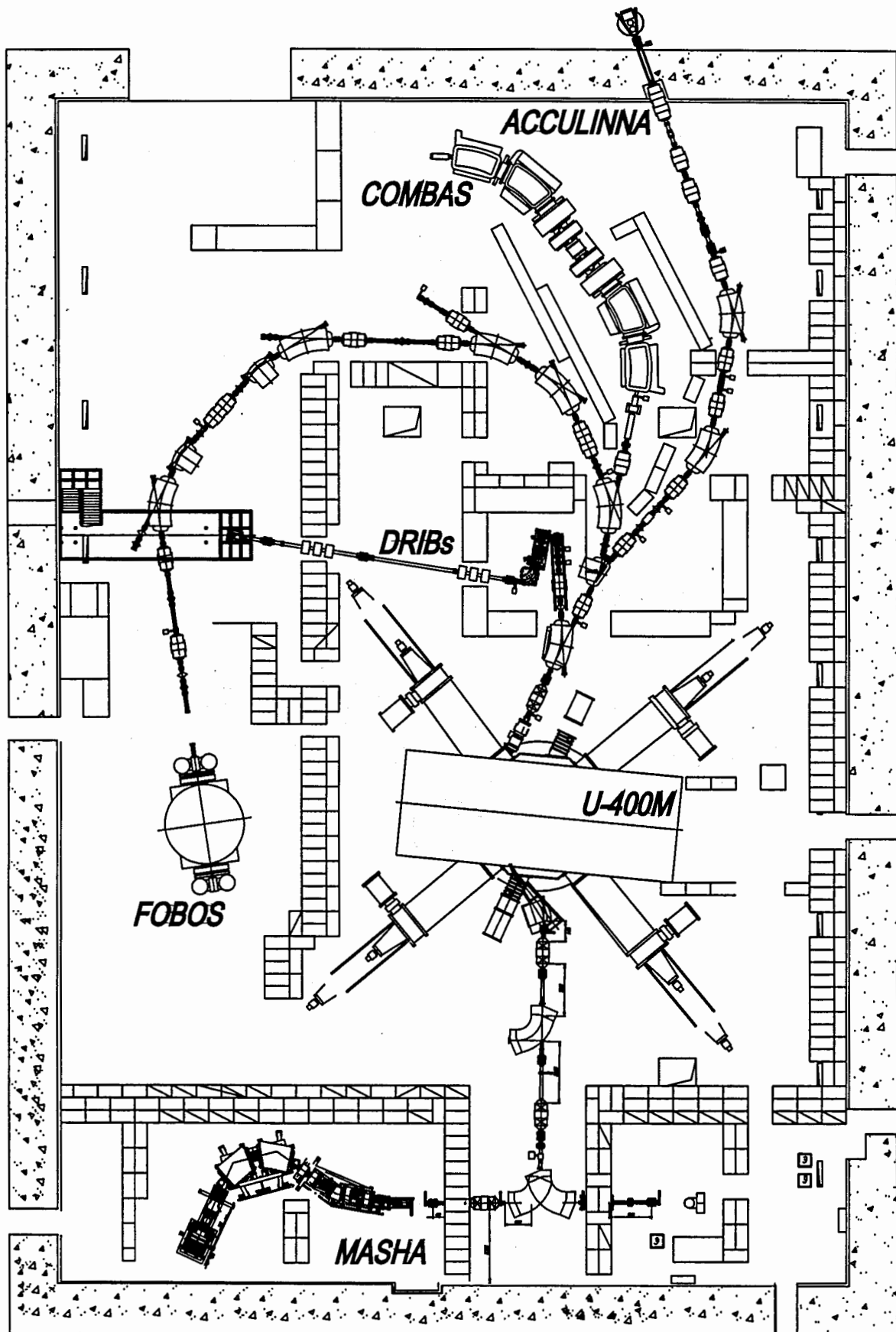


Figure 1: Schematic view of the U-400M cyclotron hall with existing experimental facilities.

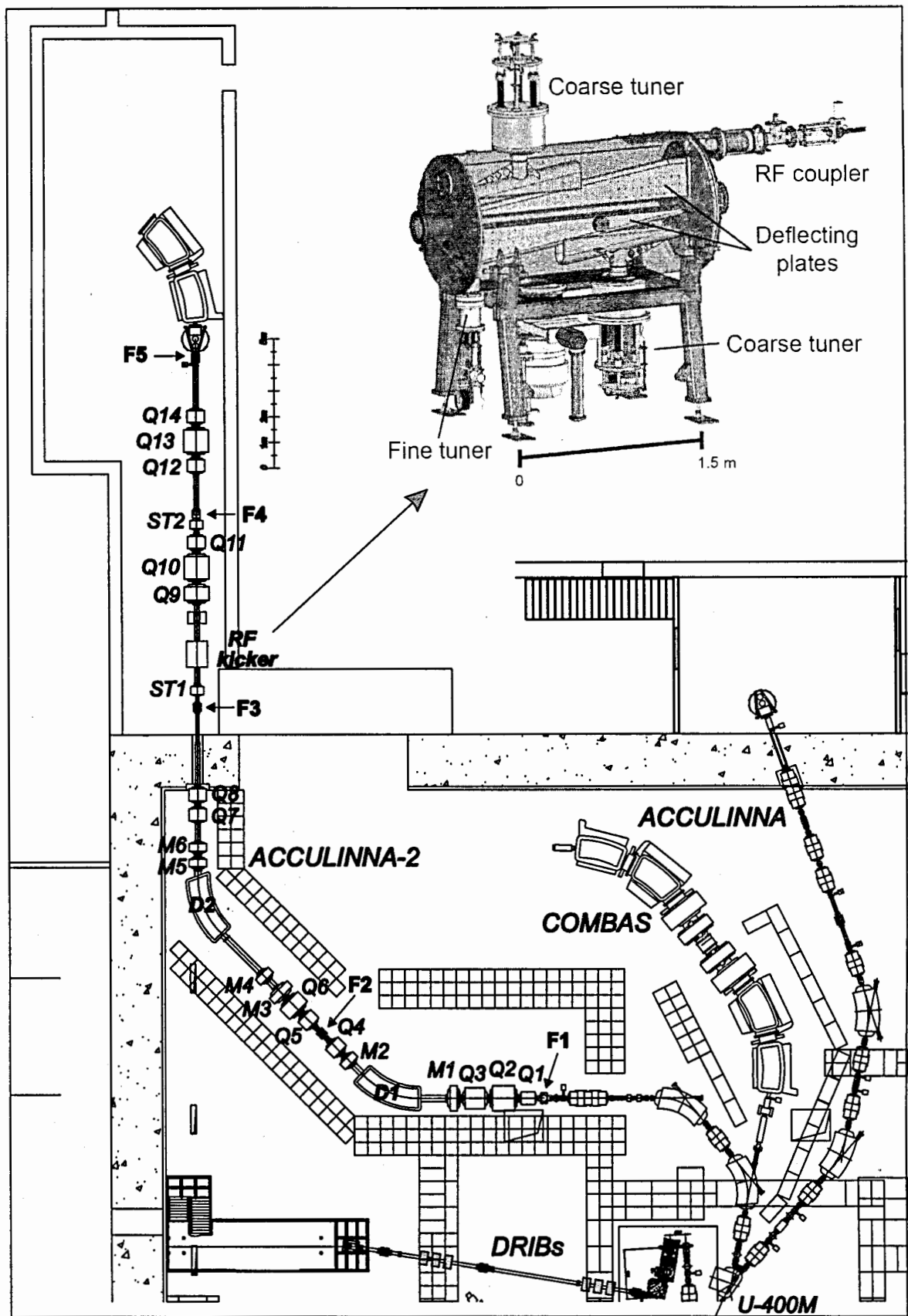


Figure 2: Schematic layout of the existing ACCULINNA and projected ACCULINNA-2 fragment separators in the U-400M hall. The inset shows the view of the MSU RF-kicker from [M. Doleans, *et al. et al. Proceedings of PAC07, Albuquerque, New Mexico, USA, p. 3585*].

5 Proposed ACCULINNA-2 technical characteristics

To meet conditions requested by the proposed scientific program the following technical features of the ACCULINNA-2 fragment separator are foreseen.

The layout of ACCULINNA-2 within the U-400M cyclotron hall is shown in Fig. 2. A beam of radioactive nuclei leaving the production target is captured by a short focusing quadrupole triplet $Q1 - Q3$ and transported through magnetic dipoles $D1 - D2$ and magnetic quadrupoles $Q4 - Q14$ up to the final focal plane F5. The F2 non-zero momentum dispersion plane is intended for the installation of a wedge-shaped energy degrader. In the achromatic focal plane F3 separation of the secondary beams with mass A and charge Z is taking place (bare nuclei are implied) according to ratio $A^{5/2}/Z^{3/2}$. This ratio arises from the cumulative effect of the A/Z separation in the F2 plane after passing $D1$ dipole and the charge/mass dependence of the energy losses in the wedge. For neutron-excess RIBs this is typically enough for preparing quite pure beams.

Proton-rich radioactive beams suffer from large amount of contaminations. To cope with this problem a vertically deflecting radio-frequency (RF) kicker is foreseen to be installed in-between F3 and Q9 [K. Yamada, T. Motobayashi and I. Tanihata, Nucl. Phys. **A746** (2004) 156c; D. Gorelov, *et al.* Proceedings of 2005 Particle Accelerator Conference, Knoxville, Tennessee, USA, p. 3880; M. Doleans, *et al.* Proceedings of PAC07, Albuquerque, New Mexico, USA, p. 3585]. The RF transverse electric field causes a phase dependent transverse deflection of ions. Technical parameters of the RF-kicker are provided in Table. 6. Two steering magnets $ST1$ and $ST2$ compensate the centroid vertical shift of the beam of interest at the vertical slit position F4 when the beam passes the RF-kicker on crest of the RF-wave. Most of the unwanted ions come to the F4 plane being beyond the vertical slit.

The most important second- and third-order aberrations in the F2 and F3 focal planes are corrected by the magnetic multipoles $M1 - M5$ having corresponding sextupole and octupole components. As a result the (x/θ_{0x}^2) , $(x/\theta_{0x}\delta_p)$, and (x/θ_{0y}^2) second order aberration coefficients become very small in the F2 and F3 planes. Smooth adjustment of focusing effect in these planes is achieved by tuning the octupole strengths of the multipoles.

Comparison of the proposed ACCULINNA-2 separator with the other fragment separators is provided in Table. 1 (see also Section 2.3 above). The main ion-optical parameters of ACCULINNA-2 are listed in Table. 2. The individual characteristics of the magnetic elements are given in Tables 3, 4, 5.

Radioactive beam envelopes calculated for a 2×2 mm² primary beam spot in F1 are shown in Fig. 3. The chosen beam spot is optimised for thermal load of the production target and

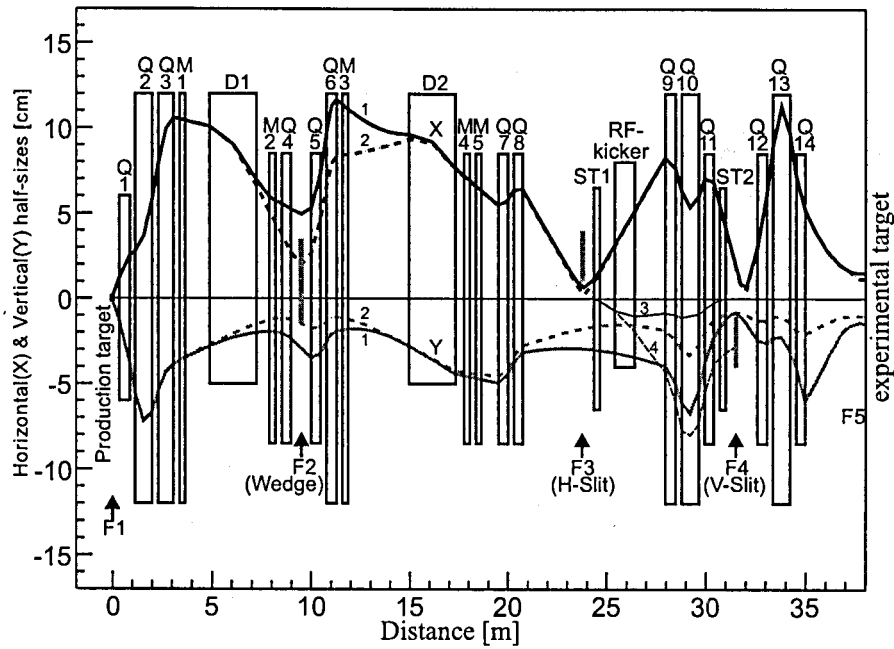


Figure 3: Envelopes of the beam in X, Y planes. Solid lines (1) are for $\delta_p = \pm 2.5\%$ and dashed ones (2) for $\delta_p = \pm 1.0\%$. Curves (3,4) show a joint action of the RF-kicker (when it is on), two steering magnets $ST1, ST2$ and three quadrupoles $Q9 - Q11$ on the centroid of a beam of interest (3) and on one of the unwanted beams which further stops at the vertical slit at $F4$ (see text).

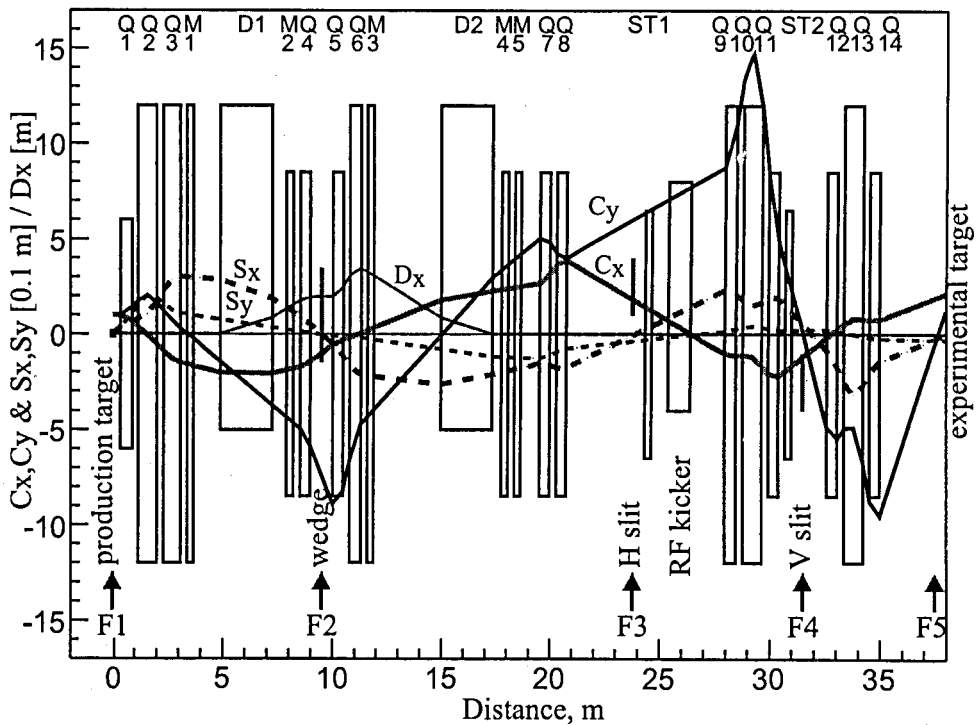


Figure 4: Main first-order trajectories cosine-like $C_x = (x/x_0)$, $C_y = (y/y_0)$ and sine-like $S_x = (x/\theta_{0x})$, $S_y = (y/\theta_{0y})$ and dispersion $D_x = (x/\delta_p)$.

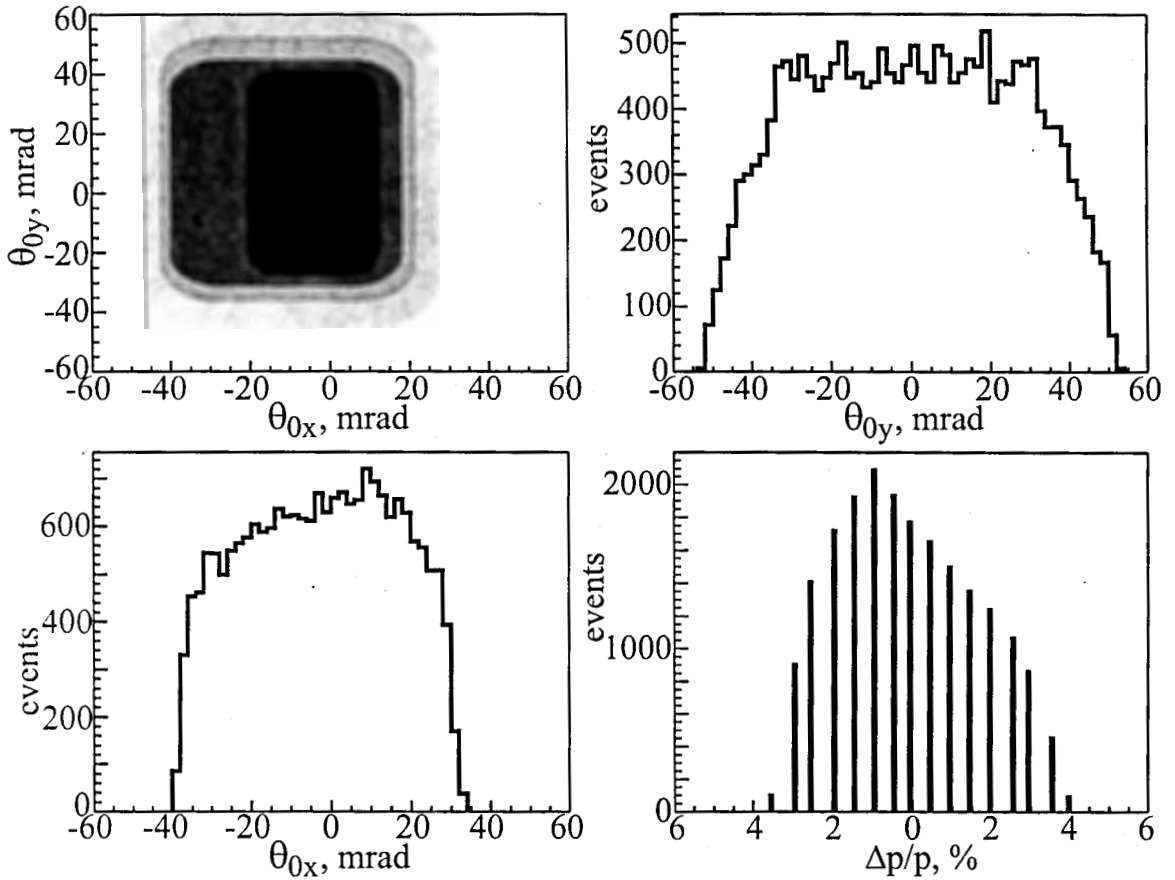


Figure 5: F1-plane: overall angular and momentum acceptances of ACCULINNA-2.

angular divergence of the primary beam. The first-order cosine- and sine-like functions and the horizontal momentum dispersion are given in Fig. 4. The envelopes were calculated with the second order accuracy by the TRANSPORT code assuming that the secondary beam is captured by the ion optical system of ACCULINNA-2 with angular divergence of ± 35 mrad in both transverse directions and momentum spread of $\pm 2.5\%$. The choice of the ACCULINNA-2 parameters provides a reasonable compromise between the separation efficiency ($B\rho_{\max}$ plus acceptances) and the facility cost.

Full ray-tracing calculations were carried out with the ZGOUBI [F. Meót and S. Valéro, *Zgoubi users' guide*, Note LNS/GT/93-12, CEA-Saclay (1993)] code taking into account realistic fringe fields of the ion-optical elements. The program performs the numerical integration of the equations of motion for ions passing the magnetic system. The overall angular ($\Delta\theta_{0x}$, $\Delta\theta_{0y}$) and momentum (δ_p) acceptances calculated from F1 to F5 are presented in Fig. 5 for the 2×2 mm² object size⁸. The corresponding transverse images in F2, F3, F4, and F5 are shown in Figures 6, 7, 8, and 9.

The purification effectiveness of the RF-kicker for proton-rich beams is demonstrated in Fig.

⁸The apertures of the ion-optical elements are taken into account.

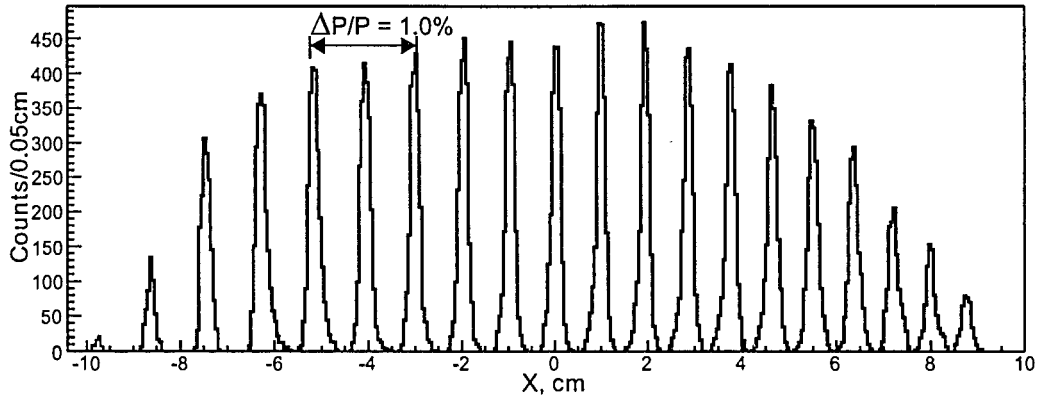
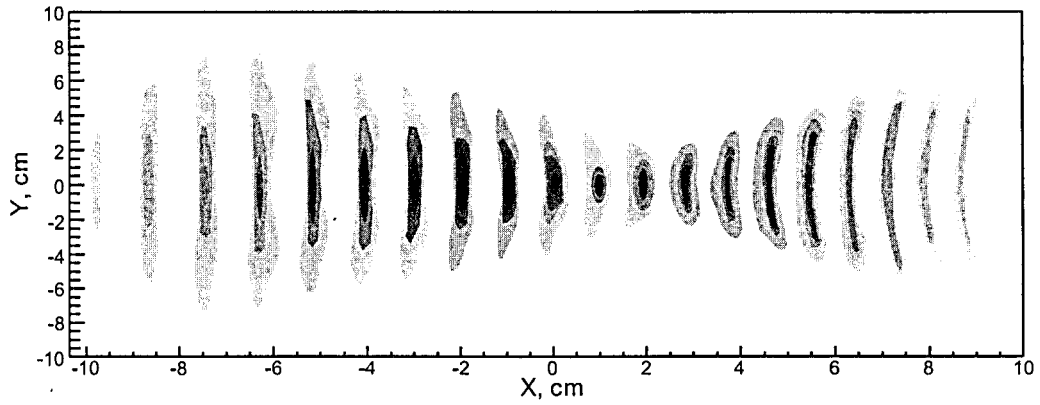


Figure 6: F2-plane: wedge plane transverse images of momentum lines with 0.5% stepping. Object size is $0.2 \times 0.2 \text{ cm}^2$.

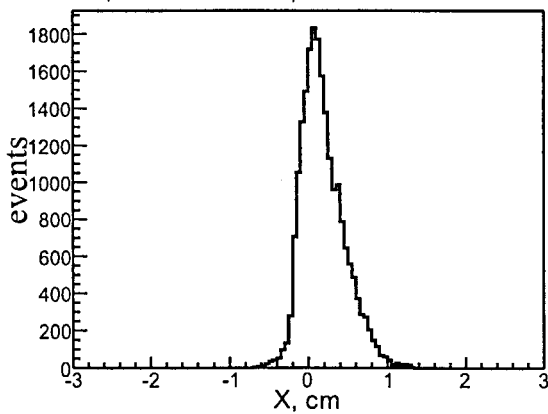
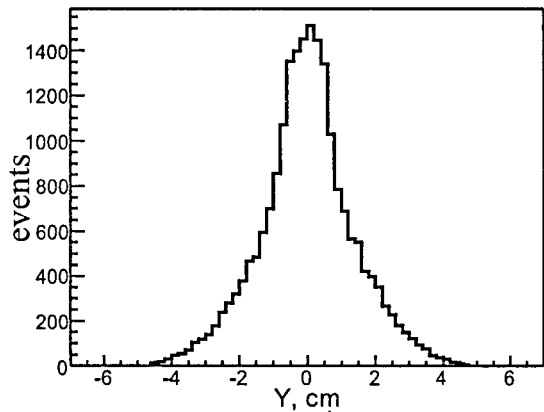
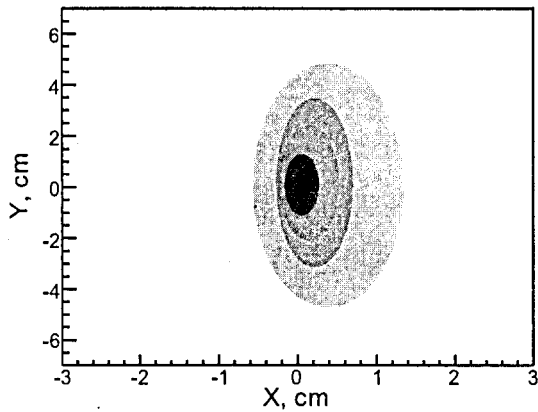


Figure 7: F3-plane: first achromatic plane image.

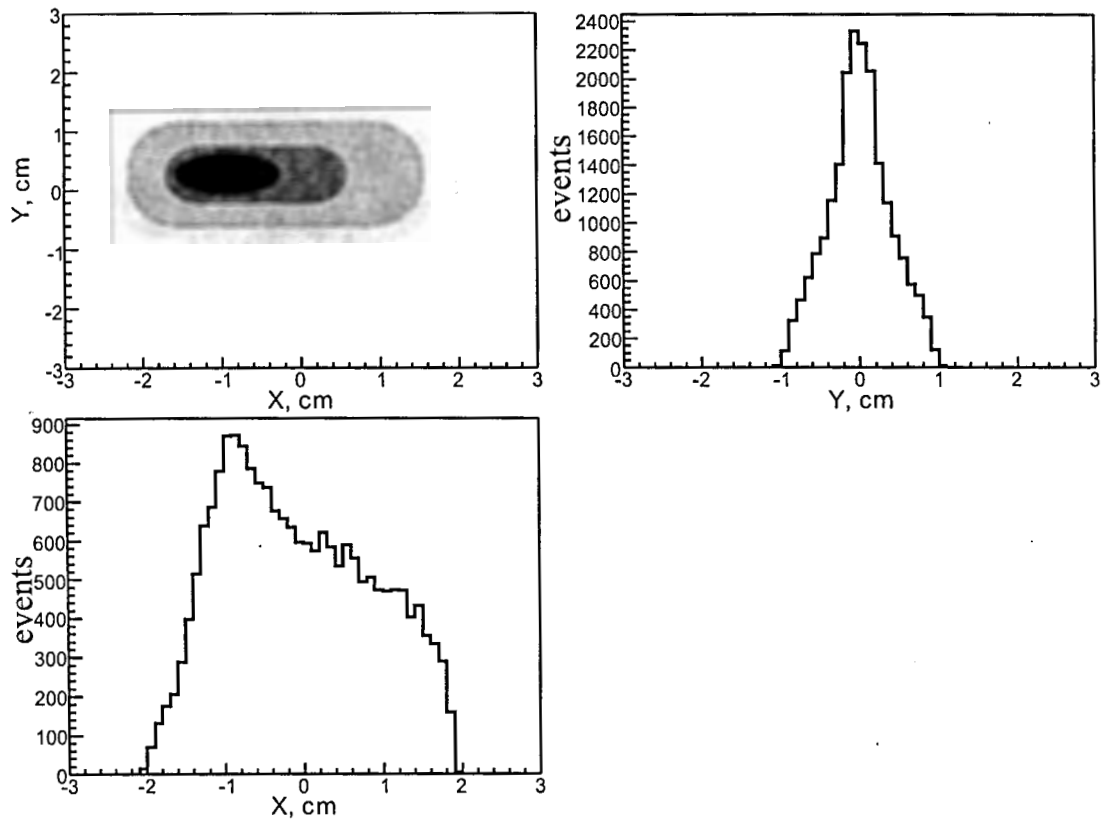


Figure 8: F4-plane: RF-kicker selection vertical slit plane image.

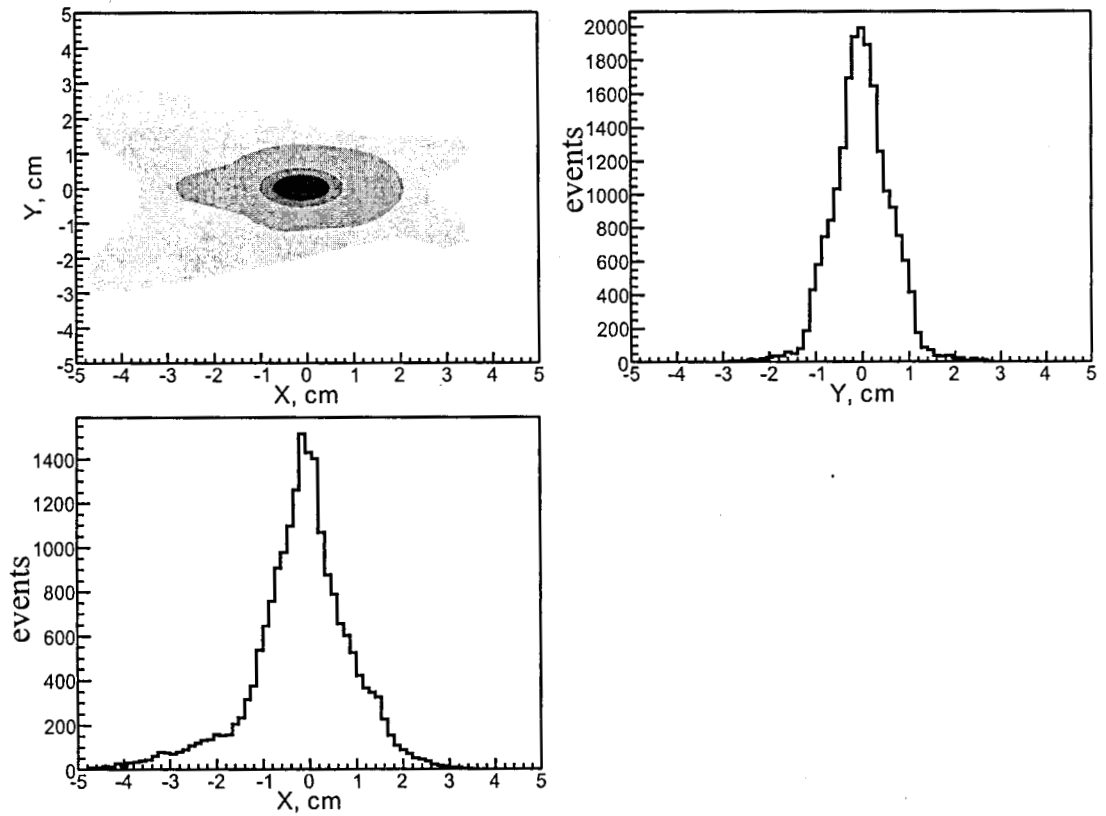


Figure 9: F5-plane: achromatic focus final image.

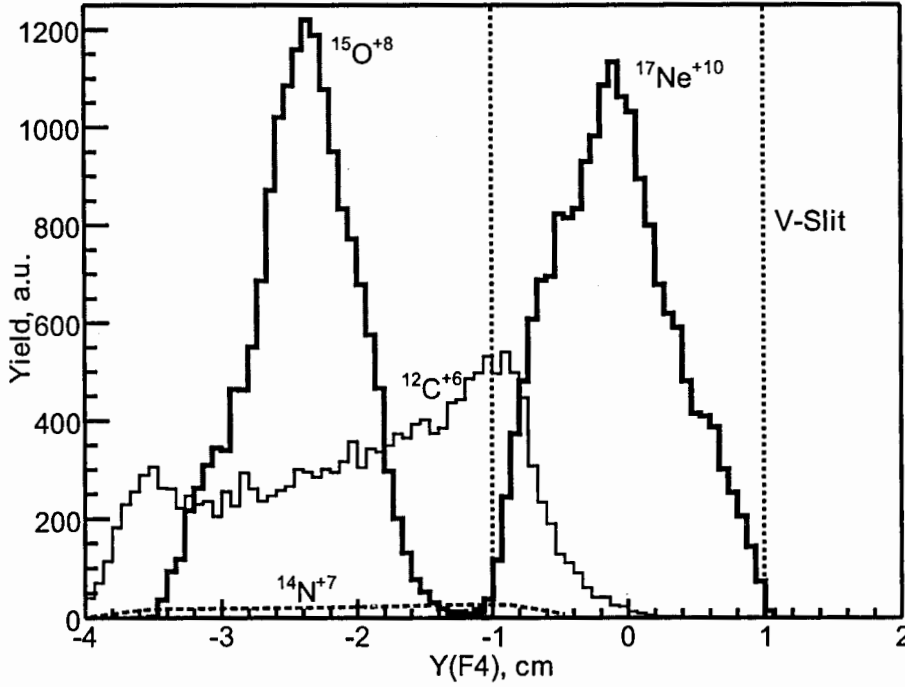


Figure 10: Beam distribution in the F4-plane. RF purification of the 40 MeV/amu ^{17}Ne proton-rich beam. Finite momentum spreads of the beams under consideration are taken into account.

10 by the example of ^{17}Ne RIB. A 40 MeV/amu ^{17}Ne beam is produced by fragmentation of 60 MeV/amu ^{20}Ne primary beam on a 150 mg/cm^2 ^9Be production target. The achromatic 185 mg/cm^2 ^9Be wedge was used in the calculations. After passing the F3 horizontal slit most of the contaminants are eliminated. The remaining ones are ^{15}O , ^{14}N , and ^{12}C . The further purification of the ^{17}Ne beam is done by the RF-kicker. At the frequency of 15 MHz and the electric field of 12.5 kV/cm on the crest of RF-wave the ions in the beam are dispersed along the vertical direction at F4 as shown in Fig. 10. In Fig. 3 the reversed paths of ^{17}Ne (curve 3) and of ^{15}O (curve 4) are presented for illustration. Now it is possible to purify the beam of ^{17}Ne up to few percent of contamination by varying the vertical slit width at F4.

5.1 The increase of the beam intensity

Development of the ACCULINNA-2 facility includes the upgrade of U-400M cyclotron to produce ^{48}Ca , ^{58}Ni , and ^{84}Kr primary beams with energies 40 – 43 MeV/amu and intensities approaching $1.0 \text{ p}\mu\text{A}$. This will result in the possibility to have 1–5 $\text{p}\mu\text{A}$ beams of 40 – 45 MeV/amu ions of ^{40}Ca , ^{40}Ar , and ^{36}S . The cyclotron upgrade includes:

1. New cryogenic ECR ion source will be installed at the cyclotron giving $\sim 30 \text{ }\mu\text{A}$ beams of $^{58}\text{Ni}^{16+}$, $^{48}\text{Ca}^{14+}$ ions and $\sim 10 \text{ }\mu\text{A}$ beam of $^{84}\text{Kr}^{20+}$ ions for injection in the cyclotron.
2. The cyclotron beam extraction system will be improved for the whole variety of the possible 30–60 MeV/amu beams.

3. The necessary shielding should be provided for the primary beam line and for the compartment of the ACCULINNA-2 production target to work with the intense beams of such ions as ${}^7\text{Li}$, ${}^{10,11}\text{B}$, ${}^{14,15}\text{N}$, ${}^{20,22}\text{Ne}$, etc. At the moment the primary beam intensities exceeding $\sim 5 \mu\text{A}$ lead to problems with radiation security.

The RIB generation in the energy range 5–60 MeV/amu will be provided by ACCULINNA-2 working with the primary beams of the upgraded U400M. The lower part of the range is suitable for resonance scattering reactions on a thick target, middle of the range is optimal for transfer reactions, and upper part is reasonable for the Coulomb dissociation studies.

5.2 The beam quality improvement

1. Introduction of the sextupole and octupole magnetic elements allows to get a good momentum resolution in the dispersive wedge plane F2 and to focus a large-emittance secondary beam into ~ 2 cm spot in the F5 plane (see Fig. 9; 2 mm beam spot in F1 is assumed).
2. Beam quality increases due to magnetic achromat being supplemented with the second beam cleaning stage — RF-kicker. A filter with maximal electric field amplitude of 15 kV/cm and frequency in the range of 13 – 15 MHz allows to purify proton-excess RIBs with velocities of up to $\beta = 0.32$ (beam energies up to 50 MeV/amu).
3. Energy resolution of the secondary ion beam on the reaction target should be better than 0.25%. The ion optical system of ACCULINNA-2 has TOF base of 14.1 m (the distance between F3 and F5 planes, see Fig. 2). This is about two times larger than ACCULINNA provides now. Modern TOF start/stop detectors (e.g., diamond or silicon planar microstrip detectors) should improve the time resolution from 400 ps, routinely achieved now, to better than 50 ps.

5.3 Expected beam properties

The availability of the primary beams at U-400M cyclotron by the moment of ACCULINNA-2 commissioning is shown in Table 7. The following beam properties are expected from the ACCULINNA-2 separator:

1. Considerable broadening of the secondary beam range. The $E = 36$ MeV/amu primary ${}^{86}\text{Kr}^{24+}$ beam can be efficiently produced by the U-400M cyclotron supplied with a new ion source (see section 4.1). Thus, RIBs with atomic numbers up to $Z = 36$ are expected to be produced and separated at ACCULINNA-2.

2. The estimated intensities of the proton-rich beams (e.g. ${}^8\text{B}$, ${}^9\text{C}$, ${}^{13}\text{O}$, ${}^{14}\text{O}$, ${}^{17}\text{Ne}$, ${}^{20}\text{Mg}$, etc.) and of neutron-rich beams (e.g. ${}^{11}\text{Li}$, ${}^{12}\text{Be}$, ${}^{14}\text{Be}$, ${}^{15}\text{B}$, ${}^{17}\text{B}$, etc.) are found in a range of $3 \times 10^4 - 3 \times 10^5 \text{ s}^{-1}$.
3. The contamination level in the beams of ${}^6\text{He}$, ${}^8\text{He}$, ${}^9\text{Li}$, ${}^{11}\text{Be}$, ${}^{12}\text{Be}$ is expected to be not more than 1 – 5% and in the beams of ${}^8\text{Be}$, ${}^9\text{C}$, ${}^{11}\text{Li}$, ${}^{13}\text{O}$, ${}^{14}\text{Be}$, ${}^{14}\text{O}$, ${}^{15}\text{B}$, ${}^{17}\text{B}$, ${}^{17}\text{Ne}$) not more than 5 – 20%.

Examples of the estimated production rates for certain RIBs of special interest are presented in Table 8. Comparison with the intensities achieved at ACCULINNA shows 1 – 3 orders of the magnitude improvement.

5.4 Broadening of the experimental opportunities

1. The secondary beam is transferred in a low-background area. In the focal plane F5 there is enough place for bulky instrumentation (zero-angle spectrometer, neutron and γ detector arrays).
2. Zero-angle spectrometer is planned at F5. This should considerably improve the cumulative energy resolution of the experiments with the observation of beam-like products or recoils.

There exists opportunity to get a good zero-angle spectrometer without much investment. The first part of the existing spectrometer COMBAS can be used in this role, providing sufficiently fine momentum resolution. The ion-optical parameters of such spectrometer are presented below. This tentative opportunity is illustrated in Fig. 2.

Magnetic rigidity	$B\rho_{\max}$	Tm	4.5
Capture solid angle	Ω_{\max}	msr	6.4
Full momentum range	$(\Delta p/p)(\max)$	%	20.0
Linear horizontal magnification			-0.4
Linear vertical magnification			-6.0
Linear momentum dispersion	D	cm/%	1.5
Linear momentum resolution	FWHM for 1 mm obj. slit		3750
Total length	L	m	7.25

3. Experimental area at F5 allows further development, including the construction of additional beam lines. This should provide comfortable conditions for running at ACCULINNA-2 several experiments simultaneously.
4. ACCULINNA-2 can be used as a “precision” beam line for stable nuclei provided by the U400M cyclotron.

6 Tentative timetable and cost estimates

The tentative work plan includes two phases: (phase 1) construction of achromatic part of fragment separator and (phase 2) installation of the RF-filter. The “core” cost of the ACCULINNA-2 fragment separator, namely, the construction of the achromatic part of the separator, including the whole set of magnets, vacuum chambers, vacuum equipment, and communications will amount to about ~ 6 MUSD. This estimate does not include the cost which one should foresee for the upgrade of the U-400M cyclotron (see Section 4.1). Development of the basic DAC system (including, first of all, the beam diagnostic system) can be estimated as ~ 1 MUSD. We plan to build and commission the main separator (phase 1) in first 3 years. After that the formulated above physical program can be started. The installation and commissioning of the RF-filter (phase 2, estimated as ~ 1 MUSD) can be done in parallel with experimental runs.

7 Participants

The following research institutions expressed interest in the construction of the new fragment separator on the base on the U-400M cyclotron:

1. Russian Research Center “The Kurchatov Institute”, Moscow, Russia (contact person: A.A. Korshennikov).
2. PTI, St.-Petersburg, Russia (contact person: V.K. Eremin).
3. INP (RAS), Moscow, Russia (contact person: V.G. Nedorezov).
4. GSI, Darmstadt, Germany (contact person: T. Aumann).
5. GANIL, Caen, France (contact person: P. Roussel-Chomaz).
6. St.-Petersburg State Univ., St.-Petersburg, Russia (contact person: K.A. Gridnev).
7. NSCL, East Lansing, Michigan, USA (contact person: W. Mittig).

References

Publications in the refereed journals

- [1] A. M. Rodin, S. I. Sidorchuk, S. V. Stepantsov, G. M. Ter-Akopian, A. S. Fomichev, R. Wolski, V. B. Galinskiy, G. B. Ivanov, I. B. Ivanova, V. A. Gorshkov, A. Yu. Lavrentyev, Yu. Ts. Oganessian,
High resolution line for secondary radioactive beams at the U400M cyclotron,
Nucl. Instr. Meth. **B126** (1996) 236-241.
- [2] A. M. Rodin, S. I. Sidorchuk, S. V. Stepantsov, G. M. Ter-Akopian, A. S. Fomichev, R. Wolski, V. B. Galinskiy, G. N. Ivanov, I. B. Ivanova, V. A. Gorshkov, A. Yu. Lavrentev, Yu. Ts. Oganessian,
High resolution beam line of the U400M cyclotron and a possibility of RIB accumulation and cooling in the K4 storage ring,
Nucl. Instr. Meth. **A391** (1997) 228-232.
- [3] G. M. Ter-Akopian, A. M. Rodin, A. S. Fomichev, S. I. Sidorchuk, S. V. Stepantsov, R. Wolski, M. L. Chelnokov, V. A. Gorshkov, A. Yu. Lavrentyev, V. I. Zagrebaev, Yu. Ts. Oganessian,
Two-neutron exchange observed in the ${}^6\text{He}+{}^4\text{He}$ reaction. Search for the "di-neutron" configuration of ${}^6\text{He}$,
Phys. Lett. **B426** (1998) 251-256.
- [4] Yu. Ts. Oganessian, V. I. Zagrebaev, J. S. Vaagen,
"Di-Neutron" Configuration of ${}^6\text{He}$
Phys. Rev. Lett. **82** (1999) 4996-4999.
- [5] V. Avdeichikov, A. S. Fomichev, B. Jakobsson, A. M. Rodin, and G. M. Ter-Akopian,
Reaction losses of light charged particles in CsI, BGO and GSO scintillators,
Nucl. Instr. Meth. **A437** (1999) 424-431.
- [6] R. Wolski, A. S. Fomichev, A. M. Rodin, S. I. Sidorchuk, S. V. Stepantsov, G. M. Ter-Akopian, M. L. Chelnokov, V. A. Gorshkov, A. Yu. Lavrentev, Yu. Ts. Oganessian, P. Roussel-Chomaz, W. Mittig, I. David,
Cluster structure of ${}^6\text{He}$ studied by means of ${}^6\text{He}+p$ reaction at 25 MeV/n energy.
Phys. Lett. **B467** (1999) 8-14.

- [7] V. Avdeichikov, A. S. Fomichev, B. Jakobsson, A. M. Rodin, and G. M. Ter-Akopian, *Rangeenergy relation, range straggling and response function of CsI(Tl), BGO and GSO(Ce) scintillators for light ions*, Nucl. Instr. Meth. **A439** (2000) 158-166.
- [8] A. A. Korshennikov, M. S. Golovkov, I. Tanihata, A. M. Rodin, A. S. Fomichev, S. I. Sidorchuk, S. V. Stepantsov, M. L. Chelnokov, V. A. Gorshkov, D. D. Bogdanov, R. Wolski, G. M. Ter-Akopian, Yu. Ts. Oganessian, W. Mittig, P. Roussel-Chomaz, H. Savajols, E. A. Kuzmin, E. Yu. Nikolskii, A. A. Ogloblin, *Superheavy Hydrogen ^5H* , Phys. Rev. Lett. **87** (2001) 092501 (4 pages).
- [9] G. M. Ter-Akopian, D. D. Bogdanov, A. S. Fomichev, Yu. Ts. Oganessian, A. M. Rodin, S. I. Sidorchuk, S. V. Stepantsov, R. Wolski, P. Roussel-Chomaz, W. Mittig, H. Savajols, M. S. Golovkov, A. A. Korshennikov, I. Tanihata, E. A. Kuzmin, E. Yu. Nikolsky, A. A. Ogloblin, *Direct Reactions Involving Exotic Nuclei ^8He and ^5H* , Acta Phys. Hung. N.S. **14** (2001) 395.
- [10] Yu. Ts. Oganessian, G. M. Ter-Akopian, D. D. Bogdanov, M. S. Golovkov, V. A. Gorshkov, A. M. Rodin, S. I. Sidorchuk, R. S. Slepnev, S. V. Stepantsov, A. S. Fomichev, M. L. Chelnokov, M. G. Itkis, E. M. Kozulin, A. A. Bogachev, N. A. Kondratiev, I. V. Korzyukov, R. Wolski, A. A. Yukhimchuk, V. V. Perevozchikov, Yu. I. Vinogradov, S. K. Grishechkin, A. M. Demin, S. V. Zlatoustovsky, A. V. Kuryakin, S. V. Filchagin, R. I. Ilkaev, F. Hanappe, T. Materna, L. Stuttge, A. H. Ninane, A. A. Korshennikov, E. Yu. Nikolsky, I. Tanihata, P. Roussel-Chomaz, W. Mittig, N. Alamanos, V. Lapoux, E. C. Pollacco, L. Nalpas, *Study of Neutron-Ultrarich Hydrogen and Helium Nuclei by Using Reactions of Radioactive Beams on Tritium Target*, Bull. Rus. Acad. Sci. Phys. **66** (2002) 676.
- [11] S. V. Stepantsov, D. D. Bogdanov, A. S. Fomichev, A. M. Rodin, S. I. Sidorchuk, R. S. Slepnev, G. M. Ter-Akopian, R. Wolski, M. L. Chelnokov, V. A. Gorshkov, Yu. Ts. Oganessian, N. Alamanos, F. Auger, V. Lapoux, G. Lobo, K. Amos, P. K. Deb, S. Karataglidis, M. S. Golovkov, A. A. Korshennikov, I. Tanihata, E. A. Kuzmin, E. Yu. Nikolskii, R. L. Kavalov,

24.5 A MeV ${}^6\text{He}+p$ Elastic and Inelastic Scattering,

Phys. Lett. **B542** (2002) 35-42.

- [12] M. S. Golovkov, Yu. Ts. Oganessian, D. D. Bogdanov, A. S. Fomichev, A. M. Rodin, S. I. Sidorchuk, R. S. Slepnev, S. V. Stepantsov, G. M. Ter-Akopian, R. Wolski, V. A. Gorshkov, M. L. Chelnokov, M. G. Itkis, E. M. Kozulin, A. A. Bogatchev, N. A. Kondratiev, I. V. Korzyukov, A. A. Yukhimchuk, V. V. Perevozchikov, Yu. I. Vinogradov, S. K. Grishechkin, A. M. Demin, S. V. Zlatoustovsky, A. V. Kuryakin, S. V. Fil'chagin, R. I. Il'kayev, F. Hanappe, T. Materna, L. Stuttge, A. H. Ninane, A. A. Korshennikov, E. Yu. Nikolskii, I. Tanihata, P. Roussel-Chomaz, W. Mittig, N. Alamanos, V. Lapoux, E. C. Pollacco, L. Nalpas,
Evidences for resonance states in ${}^5\text{H}$,
Phys. Lett. **B566** (2003) 70-75.
- [13] A. A. Yukhimchuk, V. V. Perevozchikov, V. A. Apasov, V. S. Aryutkin, Yu. I. Vinogradov, M. D. Vikharev, N. S. Ganchuk, A. N. Golubkov, S. K. Grishechkin, A. M. Demin, S. V. Zlatoustovsky, G. I. Karyakin, V. A. Klisch, A. A. Kononenko, A. A. Kukolkin, A. V. Kuryakin, V. N. Lobanov, I. L. Malkov, S. S. Matveev, V. Ya. Rozhkov, V. A. Safronov, V. M. Solyankin, V. V. Travkin, D. P. Tumkin, S. V. Filchagin, Yu. Ts. Oganessian, A. M. Rodin, D. D. Bogdanov, M. S. Golovkov, A. S. Fomichev, S. I. Sidorchuk, R. S. Slepnev, S. V. Stepantsov, G. M. Ter-Akopian, R. Wolski,
Tritium target for research in exotic neutron-excess nuclei,
Nucl. Instrum. Meth. **A513** (2003) 439.
- [14] A. A. Korshennikov, E. Yu. Nikolskii, E. A. Kuzmin, A. Ozawa, K. Morimoto, F. Tokanai, R. Kanungo, I. Tanihata, N. K. Timofeyuk, M. S. Golovkov, A. S. Fomichev, A. M. Rodin, M. L. Chelnokov, and G. M. Ter-Akopian, W. Mittig, P. Roussel-Chomaz, H. Savajols, E. Pollacco, A. A. Ogloblin, M. V. Zhukov,
Experimental Evidence for the Existence of ${}^7\text{H}$ and for a Specific Structure of ${}^8\text{He}$,
Phys. Rev. C **90** (2003) 082501.
- [15] G. V. Rogachev, V. Z. Goldberg, J. J. Kolata, G. Chubarian, D. Aleksandrov, A. Fomichev, M. S. Golovkov, Yu. Ts. Oganessian, A. Rodin, B. Skorodumov, R. S. Slepnev, G. M. Ter-Akopian, W. H. Trzaska, R. Wolski,
 $T = 5/2$ states in ${}^9\text{Li}$: Isobaric analog states of ${}^9\text{He}$,
Phys. Rev. C **67** (2003) 041603(R).

- [16] A. M. Rodin, S. V. Stepantsov, D. D. Bogdanov, M. S. Golovkov, A. S. Fomichev, S. I. Sidorchuk, R. S. Slepnev, R. Wolski, G. M. Ter-Akopian, Yu. Ts. Oganessian, A. A. Yukhimchuk, V. V. Perevozchikov, Yu. I. Vinogradov, S. K. Grishechkin, A. M. Demin, S. V. Zlatoustovsky, A. V. Kuryakin, S. V. Filchagin, R. I. Ilkaev,
Status of ACCULINNA beam line,
Nucl. Instr. Meth. **B204** (2003) 114-118.
- [17] M. S. Golovkov, L. V. Grigorenko, A. S. Fomichev, Yu. Ts. Oganessian, Yu. I. Orlov, A. M. Rodin, S. I. Sidorchuk, R. S. Slepnev, S. V. Stepantsov, G. M. Ter-Akopian, R. Wolski,
Estimates of the ${}^7\text{H}$ width and lower decay energy limit,
Phys. Lett. **B588** (2004) 163.
- [18] S. I. Sidorchuk, D. D. Bogdanov, A. S. Fomichev, M. S. Golovkov, Yu. Ts. Oganessian, A. M. Rodin, R. S. Slepnev, S. V. Stepantsov, G. M. Ter-Akopian, R. Wolski, A. A. Korshennikov, E. Yu. Nikolskii, A. A. Yukhimchuk, V. V. Perevozchikov, Yu. I. Vinogradov, F. Hanappe, T. Materna, L. Stuttge, A. H. Ninane, W. Mittig, P. Roussel-Chomaz,
Experimental Study of ${}^4\text{H}$ in the reactions ${}^2\text{H}(t,p)$ and ${}^3\text{H}(t,d)$,
Phys. Lett. **B594** (2004) 54-60.
- [19] S. V. Stepantsov, M. S. Golovkov, A. S. Fomichev, A. M. Rodin, S. I. Sidorchuk, R. S. Slepnev, G. M. Ter-Akopian, M. L. Chelnokov, V. A. Gorshkov, Yu. Ts. Oganessian, R. Wolski, A. A. Korshennikov, E. Yu. Nikolskii, I. Tanihata,
 ${}^5\text{H}$ and ${}^5\text{He}$ nuclear systems studied by means of the ${}^6\text{He}+{}^2\text{H}$ reaction,
Nucl. Phys. **A738** (2004) 436.
- [20] M. S. Golovkov, L. V. Grigorenko, A. S. Fomichev, S. A. Krupko, Yu. Ts. Oganessian, A. M. Rodin, S. I. Sidorchuk, R. S. Slepnev, S. V. Stepantsov, G. M. Ter-Akopian, R. Wolski, M. G. Itkis, A. A. Bogatchev, N. A. Kondratiev, E. M. Kozulin, A. A. Korshennikov, E. Yu. Nikolskii, P. Roussel-Chomaz, W. Mittig, R. Palit, V. Bouchat, V. Kinnard, T. Materna, F. Hanappe, O. Dorvaux, L. Stuttgé, A. A. Yukhimchuk, V. V. Perevozchikov, Yu. I. Vinogradov, S. K. Grishechkin, S. V. Zlatoustovskiy, V. Lapoux, R. Raabe, L. Nalpas,
Observation of excited states in ${}^5\text{H}$,
Phys. Rev. Lett. **93** (2004) 262501.
- [21] M. S. Golovkov, L. V. Grigorenko, A. S. Fomichev, S. A. Krupko, Yu. Ts. Oganessian, A. M. Rodin, S. I. Sidorchuk, R. S. Slepnev, S. V. Stepantsov, G. M. Ter-Akopian, R. Wolski, M. G. Itkis, A. A. Bogatchev, N. A. Kondratiev, E. M. Kozulin, A. A. Korshennikov,

E. Yu. Nikolskii, P. Roussel-Chomaz, W. Mittig, R. Palit, V. Bouchat, V. Kinnard, T. Materna, F. Hanappe, O. Dorvaux, L. Stuttgé, A. A. Yukhimchuk, V. V. Perevozchikov, Yu. I. Vinogradov, S. K. Grishechkin, S. V. Zlatoustovskiy, V. Lapoux, R. Raabe, L. Nalpas,

Correlation studies of the ^5H spectrum,

Phys. Rev. C **72** (2005) 064612.

- [22] M. S. Golovkov, L. V. Grigorenko, A. S. Fomichev, A. V. Gorshkov, V. A. Gorshkov, S. A. Krupko, Yu. Ts. Oganessian, A. M. Rodin, S. I. Sidorchuk, R. S. Slepnev, S. V. Stepantsov, G. M. Ter-Akopian, R. Wolski, A. A. Korsheninnikov, E. A. Kuzmin, E. Yu. Nikolskii, B. G. Novatskii, D. N. Stepanov, P. Roussel-Chomaz, W. Mittig,

New insight into the low-energy ^9He spectrum,

Phys. Rev. C **76** (2007) 021605(R).

- [23] K. Miernik, W. Dominik, H. Czyrkowski, R. Dabrowski, A. Fomichev, M. Golovkov, Z. Janas, W. Kusmierz, M. Pfützner, A. Rodin, S. Stepantsov, R. Slepnev, G. M. Ter-Akopian, and R. Wolski,

Optical Time Projection Chamber for imaging nuclear decays,

Nucl. Instr. Meth. **A581** (2007) 194197.

- [24] M. S. Golovkov, L. V. Grigorenko, G. M. Ter-Akopian, A. S. Fomichev, Yu. Ts. Oganessian, V. A. Gorshkov, S. A. Krupko, A. M. Rodin, S. I. Sidorchuk, R. S. Slepnev, S. V. Stepantsov, R. Wolski, D. Y. Pang, V. Chudoba, A. A. Korsheninnikov, E. A. Kuzmin, E. Yu. Nikolskii, B. G. Novatskii, D. N. Stepanov, P. Roussel-Chomaz, W. Mittig, A. Ninane, F. Hanappe, L. Stuttgé, A. A. Yukhimchuk, V. V. Perevozchikov, Yu. I. Vinogradov, S. K. Grishechkin, S. V. Zlatoustovskiy,

Possible novel interpretation of the ^8He and ^{10}He spectra studied in the (t,p) reaction,

arXiv:0804.0310v1, submitted to Phys. Lett. B.

- [25] L. V. Grigorenko, M. S. Golovkov, G. M. Ter-Akopian, A. S. Fomichev, Yu. Ts. Oganessian, V. A. Gorshkov, S. A. Krupko, A. M. Rodin, S. I. Sidorchuk, R. S. Slepnev, S. V. Stepantsov, R. Wolski, D. Y. Pang, V. Chudoba, A. A. Korsheninnikov, E. A. Kuzmin, E. Yu. Nikolskii, B. G. Novatskii, D. N. Stepanov, P. Roussel-Chomaz, W. Mittig, A. Ninane, F. Hanappe, L. Stuttgé, A. A. Yukhimchuk, V. V. Perevozchikov, Yu. I. Vinogradov, S. K. Grishechkin, S. V. Zlatoustovskiy,

Soft dipole mode in ^8He ,

Part. and Nucl. Lett., in print.

Publications in the conference proceedings

- [26] R. Kalpakchieva, V. Z. Maidikov, V. N. Melnikov, Yu. Ts. Oganessian, Yu. E. Penionzhkevich, A. M. Rodin, S. I. Sidorchuk, S. V. Stepantsov, N. I. Tarantin, G. M. Ter-Akopian, *Project of a High Resolution Beam Line at the U400M Cyclotron for Studies of Exotic Nuclear Systems and Reactions*,
Int. Workshop on Experimental Perspectives with Radioactive Nuclear Beams. LNL Padova, November 14-16 1994, IPN, Orsay, 1994, France 119-123.
- [27] A. M. Rodin, S. I. Sidorchuk, S. V. Stepantsov, G. M. Ter-Akopian, A. S. Fomichev, R. Wolski, V. B. Galinskiy, G. B. Ivanov, I. B. Ivanova, V. A. Gorshkov, A. Yu. Lavrentyev, Yu. Ts. Oganessian,
High resolution beam line of the U400M cyclotron and a possibility of RIB accumulation and cooling in the K4 storage ring,
Nucl. Phys. **A626** (1997) 567c-574c.
- [28] G. M. Ter-Akopian, A. M. Rodin, A. S. Fomichev, S. I. Sidorchuk, S. V. Stepantsov, R. Wolski, M. L. Chelnokov, V. A. Gorshkov, A. Yu. Lavrentyev, V. B. Galinskiy, G. B. Ivanov, I. B. Ivanova, V. I. Zagrebaev, Yu. Ts. Oganessian,
Production of a high quality ${}^6\text{He}$ beam and two-neutron exchange observed in the ${}^6\text{He} + {}^4\text{He}$ reaction,
Heavy Ion Physics, VI Int. School-Seminar Dubna 1997. Yu. Ts. Oganessian and R. Kalpakchieva (Eds) World Scientific, Singapore 1998, p.105-113.
- [29] M. S. Golovkov, A. A. Korshennikov, I. Tanihata, D. D. Bogdanov, M. L. Chelnokov, A. S. Fomichev, V. A. Gorshkov, Yu. Ts. Oganessian, A. M. Rodin, S. I. Sidorchuk, S. V. Stepantsov, G. M. Ter-Akopian, R. Wolski, W. Mittig, P. Roussel-Chomaz, H. Savajols, E. A. Kuzmin, E. Yu. Nikolskii, B. G. Novatskii, A. A. Ogloblin,
Spectroscopy of ${}^7\text{He}$ and Superheavy Hydrogen Isotope ${}^5\text{H}$,
Proc. of Int. Conf. "Nuclear Structure and Related Topics" JINR, Dubna, Russia, June 6-10 (2000).
- [30] M. S. Golovkov, A. A. Korshennikov, I. Tanihata, D. D. Bogdanov, M. L. Chelnokov, A. S. Fomichev, V. A. Gorshkov, Yu. Ts. Oganessian, A. M. Rodin, S. I. Sidorchuk, S. V. Stepantsov, G. M. Ter-Akopian, R. Wolski, W. Mittig, P. Roussel-Chomaz, H. Savajols, E. A. Kuzmin, E. Yu. Nikolskii, B. G. Novatskii, A. A. Ogloblin,
Spectroscopy of ${}^7\text{He}$ and Superheavy Hydrogen Isotope ${}^5\text{H}$,
Phys. At. Nucl. **64** (2001) 1244-1248.

- [31] A. A. Korshennikov, M. S. Golovkov, A. Ozawa, K. Yoshida, I. Tanihata, Z. Fulop, K. Kusaka, K. Morimoto, H. Otsu, H. Petruscu, F. Tokanai, D. D. Bogdanov, M. L. Chelnokov, A. S. Fomichev, V. A. Gorshkov, Yu. Ts. Oganessian, A. M. Rodin, S. I. Sidorchuk, S. V. Stepantsov, G. M. Ter-Akopian, R. Wolski, W. Mittig, P. Roussel-Chomaz, H. Savajols, E. A. Kuzmin, E. Yu. Nikolsky, B. G. Novatsky, A. A. Ogloblin,
Superheavy Hydrogen ^5H and Spectroscopy of ^7He ,
Phys. At. Nucl. **65** (2002) 664-668.
- [32] R. Wolski, A. S. Fomichev, A. M. Rodin, S. I. Sidorchuk, S. V. Stepantsov, G. M. Ter-Akopian, Yu. Ts. Oganessian, W. Mittig, P. Roussel-Chomaz, N. Alamanos, V. Lapoux, R. Raabe,
Interaction of ^8He Nuclei with alpha Particles and Protons at a Beam Energy of 26 MeV/n,
Nucl. Phys. **A701** (2002) 29c.
- [33] G. M. Ter-Akopian, D. D. Bogdanov, A. S. Fomichev, M. S. Golovkov, Yu. Ts. Oganessian, A. M. Rodin, S. I. Sidorchuk, R. S. Slepnev, S. V. Stepantsov, R. Wolski, V. A. Gorshkov, M. L. Chelnokov, A. A. Korshennikov, E. Yu. Nikolskii, I. Tanihata, F. Hanappe, T. Materna, L. Stuttge, A. H. Ninane,
Resonance States of Hydrogen Nuclei ^4H and ^5H Obtained in Transfer Reactions with Exotic Beams,
Phys. At. Nucl. **66** (2003) 1544-1551.
- [34] R. Wolski, S. I. Sidorchuk, G. M. Ter-Akopian, A. S. Fomichev, A. M. Rodin, S. V. Stepantsov, W. Mittig, P. Roussel-Chomaz, H. Savajols, N. Alamanos, F. Auger, V. Lapoux, R. Raabe, Yu. M. Tchuvilsky, K. Rusek,
Elastic scattering of ^8He on ^4He and ^4n system,
Nucl. Phys. **A722** (2003) 55c-60c.
- [35] W. Mittig, H. Savajols, C. E. Demonchy, L. Giot, P. Roussel-Chomaz, H. Wang, G. Ter-Akopian, A. Fomichev, M. S. Golovkov, S. Stepantsov, R. Wolski, N. Alamanos, A. Drouart, A. Gillibert, V. Lapoux, E. Pollacco,
New target and detection methods: active detectors,
Nucl. Phys. **A722** (2003) 10c.
- [36] S. I. Sidorchuk, D. D. Bogdanov, A. S. Fomichev, M. S. Golovkov, Yu. Ts. Oganessian, A. M. Rodin, R. S. Slepnev, S. V. Stepantsov, G. M. Ter-Akopian, R. Wolski, V. A. Gorshkov, M. L. Chelnokov, M. G. Itkis, E. M. Kozulin, A. A. Bogatchev, N. A. Kondratiev, I. V. Korzyukov, A. A. Korshennikov, E. Yu. Nikolskii, I. Tanihata,

Resonance states of hydrogen nuclei ^4H and ^5H obtained in transfer reactions with exotic beams,

Nucl. Phys. **A719** (2003) 229c-232c.

- [37] G. M. Ter-Akopian, Yu. Ts. Oganessian, M. G. Itkis, G. G. Gulbekian, D. D. Bogdanov, A. S. Fomichev, M. S. Golovkov, A. M. Rodin, S. V. Stepantsov, R. Wolski, *Radioactive ion beam research made in Dubna,*
Nucl. Phys. **A734** (2004) 295.
- [38] R. Wolski, P. Roussel-Chomaz, S. I. Sidorchuk, G. M. Ter-Akopian, *Search for extremely neutron rich systems,*
Nucl. Phys. **A738** (2004) 431-435.
- [39] G. V. Rogachev, A. Aprahamian, F. D. Becchetti, P. Boutachkov, Y. Chen, G. Chubarian, P. A. DeYoung, A. Fomichev, V. Z. Goldberg, M. S. Golovkov, J. J. Kolata, Yu. Ts. Oganessian, G. F. Peaslee, M. Quinn, A. Rodin, B. B. Skorodumov, R. S. Slepnev, G. Ter-Akopian, W. H. Trzaska, A. Wohr, R. Wolski, *Structure of exotic ^7He and ^9He ,*
Nucl. Phys. **A746** (2004) 229c.
- [40] G. M. Ter-Akopian, A. S. Fomichev, M. S. Golovkov, L. V. Grigorenko, S. A. Krupko, Yu. Ts. Oganessian, A. M. Rodin, S. I. Sidorchuk, R. S. Slepnev, S. V. Stepantsov, R. Wolski, A. A. Korshennikov, E. Yu. Nikolskii, P. Roussel-Chomaz, W. Mittig, R. Palit, V. Bouchat, V. Kinnard, T. Materna, F. Hanappe, O. Dorvaux, L. Stuttge, C. Angulo, V. Lapoux, R. Raabe, L. Nalpas, A. A. Yukhimchuk, V. V. Perevozchikov, Yu. I. Vinogradov, S. K. Grishechkin, S. V. Zlatoustovskii, *New insights into the resonance states of ^5H and ^5He ,*
Eur. Phys. J. **A 25**, Supplement 1 (2005) 315.
- [41] W. Mittig, C. E. Demonchy, H. Wang, P. Roussel-Chomaz, B. Jurado, M. Gelin, H. Savajols, A. Fomichev, A. Rodin, A. Gillibert, A. Obertelli, M. D. Cortina-Gil, M. Caamano, M. Chartier, and R. Wolski, *Reactions induced beyond the dripline at low energy by secondary beams,*
Eur. Phys. J. **A direct** (2005), DOI: 10.1140/epjad/i2005-06-138-5.
- [42] R. Wolski, M. S. Golovkov, L. V. Grigorenko, A. S. Fomichev, A. V. Gorshkov, V. A. Gorshkov, S. A. Krupko, Yu. Ts. Oganessian, A. M. Rodin, S. I. Sidorchuk, R. S. Slepnev, S. V. Stepantsov, G. M. Ter-Akopian, A. A. Korshennikov, E. Yu. Nikolskii, V. A.

- Kuzmin, B. G. Novatskii, D. N. Stepanov, P. Roussel-Chomaz, W. Mittig,
Spectroscopy of ^9He , Quasi-free Scattering $^6\text{He}+^4\text{He}$,
 TOURS SYMPOSIUM ON NUCLEAR PHYSICS VI. AIP Conference Proceedings, **891**
 (2007) 226-234.
- [43] M. S. Golovkov, L. V. Grigorenko, A. S. Fomichev, A. V. Gorshkov, V. A. Gorshkov, S. A. Krupko, Yu. Ts. Oganessian, A. M. Rodin, S. I. Sidorchuk, R. S. Slepnev, S. V. Stepantsov, G. M. Ter-Akopian, R. Wolski, A. A. Korsheninnikov, E. Yu. Nikolskii, V. A. Kuzmin, B. G. Novatskii, D. N. Stepanov, P. Roussel-Chomaz, W. Mittig,
First Results of a $^8\text{He}+d$ Experiment,
 INTERNATIONAL SYMPOSIUM ON EXOTIC NUCLEI. AIP Conference Proceedings,
912 (2007) 32-42.
- [44] M. S. Golovkov, L. V. Grigorenko, A. S. Fomichev, A. V. Gorshkov, V. A. Gorshkov, S. A. Krupko, Yu. Ts. Oganessian, A. M. Rodin, S. I. Sidorchuk, R. S. Slepnev, S. V. Stepantsov, G. M. Ter-Akopian, R. Wolski, A. A. Korsheninnikov, E. Yu. Nikolskii, P. Roussel-Chomaz, W. Mittig, V. A. Kuzmin, B. G. Novatskii, D. N. Stepanov,
Properties of low-lying ^9He state,
 Eur. Phys. J. Special Topics, **150** (2007) 23-26.
- [45] G. M. Ter-Akopian, A. S. Fomichev, M. S. Golovkov, L. V. Grigorenko, S. A. Krupko, Yu. Ts. Oganessian, A. M. Rodin, S. I. Sidorchuk, R. S. Slepnev, S. V. Stepantsov, R. Wolski, A. A. Korsheninnikov, E. Yu. Nikolskii, P. Roussel-Chomaz, W. Mittig, V. A. Kuzmin, B. G. Novatskii, D. N. Stepanov,
Neutron excess nuclei of hydrogen and helium at ACCULINNA,
 Eur. Phys. J. Special Topics, **150** (2007) 61-66.
- [46] S. I. Sidorchuk, A. S. Fomichev, M. S. Golovkov, L. V. Grigorenko, V. A. Gorshkov, A. V. Gorshkov, S. A. Krupko, Yu. Ts. Oganessian, A. M. Rodin, R. S. Slepnev, S. V. Stepantsov, G. M. Ter-Akopian, R. Wolski, A. A. Korsheninnikov, E. Yu. Nikolskii, P. Roussel-Shomaz, W. Mittig, E. A. Kuzmin, B. G. Novatskii, D. N. Stepanov,
Experimental Study of 3-body correlations in ^6He in the Reaction of Quasi-Free Knockout $^6\text{He}(^6\text{He},2\alpha)2n,$
 Proc. 11-th Int. Conf. on Reaction Mechanisms, Varenna (Italy), June 2006. E. Gadioly, Ed., Università degli Studi di Milano, Ricerca Scientifica ed Educazione Permanente, Supplemento **126** (2007) 459.

- [47] S. I. Sidorchuk, M. S. Golovkov, L. V. Grigorenko, A. S. Fomichev, V. A. Gorshkov, A. V. Gorshkov, S. A. Krupko, Yu. Ts. Oganessian, A. M. Rodin, R. S. Slepnev, S. V. Stepantsov, G. M. Ter-Akopian, R. Wolski, A. A. Korshennikov, E. Yu. Nikolskii, E. A. Kuzmin, B. G. Novatskii, D. N. Stepanov, P. Roussel-Shomaz, W. Mittig,
Three-Body Correlations in ${}^6\text{He}$ Revealed in the Quasi-Free Knockout Reaction ${}^4\text{He}({}^6\text{He}, 2\alpha)2n$,
Int. Symp. on Exotic Nuclei EXON-2006 Khanty-Mansiysk, Russia, 2006. AIP Conference Proc., **912** (2007) 43-52.
- [48] K. Miernik, W. Dominik, Z. Janas, M. Pfützner, C. Bingham, H. Czyrkowski, M. Ćwiok, I. G. Darby, R. Dabrowski, A. Fomichev, T. Gintei, M. Golovkov, R. Grzywacz, M. Karny, A. Korgul, W. Kuśmierz, S. Liddick, M. Rajabali, A. Rodin, K. Rykaczewski, S. Stepantsov, R. Slepnev, A. Stolz, G. M. Ter-Akopian, R. Wolski,
Imaging nuclear decays with Optical Time Projection Chamber,
PROTON EMITTING NUCLEI AND RELATED TOPICS: International Conference-PROCON 2007. AIP Conference Proceedings, **961** (2007) 307-309.

Table 1: Characteristics of in-flight RIB separators. The RIB energy E is in MeV/amu, $\delta_P = \Delta P/P$ is the momentum acceptance, and $P/\Delta P$ is the first-order momentum resolution (1 mm object size is assumed).

		ACC	ACC-2	LISE3	^a A1900	RIPS	^a BigRIPS	FRS	^a SuperFRS
		FLNR, JINR		GANIL	MSU		RIKEN		GSI/FAIR
$\Delta\Omega$	msr	0.9	5.8	1.0	8.0	5.0	8.0	0.32	5.0
δ_P	%	2.5	6.0	5.0	5.5	6.0	6.0	2.0	5.0
$P/\Delta P$		1000	2000	2200	2915	1500	3300	8600	3050
$B\rho_{max}$	Tm	3.2	3.9	3.2-4.3	6.0	5.76	9.0	18	18
Lengths	m	21	38	19(42)	35	21	77	74	140
E_{min}		10	5	40	110	50		220	
E_{max}		40	50	80	160	90	350	1000	1500

^aSuper-conducting magnets are used in the ion-optical system.

Table 2: Main ion-optical parameters of ACCULINNA-2.

Primary beam spot size on production target	F1	0.2	cm
Maximum momentum acceptance		6.0	%
θ_{0x} angular acceptance		65	mrad
θ_{0y} angular acceptance		90	mrad
X momentum dispersion	F1 → F2	2.0	cm/% $B\rho$
θ_x angular momentum dispersion	F1 → F2	0.3	mrad/% $B\rho$
X magnification	F1 → F2	-1.0	
Y magnification	F1 → F2	-7.4	
X momentum dispersion	F2 → F3	3.5	cm/% $B\rho$
X magnification	F2 → F3	-1.8	
Y magnification	F2 → F3	-1.8	
X magnification	F1 → F3	1.8	
Y magnification	F1 → F3	6.1	
X magnification	F1 → F5	2.1	
Y magnification	F1 → F5	1.2	
Length	F1 → F2	9.51	m
Length	F2 → F3	14.35	m
Length	F3 → F5	14.11	m
Length	F1 → F5	37.97	m

Table 3: Ion-optical parameters of ACCULINNA-2 magnetic dipoles $D1$, $D2$ and steering (correcting) magnets $ST1$, $ST2$.

Value		units	$D1$	$D2$	$ST1, ST2$
Bending direction			horizontal	horizontal	vertical
Type			sector	sector	rectangular
Gap height	$2h$	cm	10	10	10
Bending mean radius	R	m	3.0	3.0	
Bending field	B_{\max}	T	1.3	1.3	0.05
Length	L_{eff}	m	2.356	2.356	0.3
Working width	$2w$	cm	24	24	24
Bending angle	Φ	dgr	45	45	
Entrance angle	τ_{entr}	dgr	0	0	0
Exit angle	τ_{exit}	dgr	0	20	0

Table 4: Ion-optical parameters of ACCULINNA-2 magnetic quadrupoles.

Value	units	$Q1$	$Q2, 10, 13$	$Q3$	$Q4, 5, 7, 8, 11, 12, 14$	$Q6, 9$	
Aperture	$2r$	cm	12	24	24	17	24
Length	L_{eff}	cm	54.2	85.7	76.9	45.9	52.3
Field gradient	G_{\max}	T/m	9.2	7.6	3.8	10.0	6.2

Table 5: Ion-optical parameters of ACCULINNA-2 magnetic multipoles.

Multipole	Aperture $2r$ (cm)	Length L_{eff} (cm)	Sextupole strength S_{\max} (T/m ²)	Octupole strength S_{\max} (T/m ³)
$M1, M3$	24	28.6	1.9	8.2
$M2, M4$	17	28.6	20.0	
$M5$	17	28.6	7.5	32.0

Table 6: Ion-optical parameters of ACCULINNA-2 RF-kicker.

Electrode vertical gap	$2h$	cm	7
Electrode width	$2w$	cm	15
Electrode length	L	cm	100
Electric field amplitude	E_{\max}	kV/cm	15
Frequency	f	MHz	13 – 15

Table 7: U-400M cyclotron beams planned to be delivered to ACCULINNA-2.

Beam	Energy (MeV/amu)	Intensity (pμA)
${}^7\text{Li}^{2+}$	34	10
${}^{10}\text{B}^{3+}$	39	10
${}^{11}\text{B}^{3+}$	32	10
${}^{12}\text{C}^{4+}$	48	10
${}^{13}\text{C}^{4+}$	41	10
${}^{14}\text{N}^{5+}$	56	10
${}^{15}\text{N}^{5+}$	49	10
${}^{16}\text{O}^{5+}$	42	10
${}^{16}\text{O}^{6+}$	62	5 – 10
${}^{18}\text{O}^{5+}$	33	10
${}^{18}\text{O}^{6+}$	48	5 – 10 ^a
${}^{20}\text{Ne}^{7+}$	53	10
${}^{22}\text{Ne}^{7+}$	44	10
${}^{32}\text{S}^{11+}$	52	10
${}^{36}\text{S}^{12+}$	48	5 – 10 ^b
${}^{36}\text{Ar}^{12+}$	39	10
${}^{36}\text{Ar}^{13+}$	57	5 ^c
${}^{40}\text{Ar}^{13+}$	46	5
${}^{40}\text{Ca}^{14+}$	53	5
${}^{48}\text{Ca}^{15+}$	42	2 – 3 ^d
${}^{58}\text{Ni}^{19+}$	47	2
${}^{58}\text{Ni}^{20+}$	52	1
${}^{64}\text{Ni}^{20+}$	43	1
${}^{78}\text{Kr}^{24+}$	41	1

^aThis beam is required for getting secondary beams of ${}^{14}\text{Be}$ and ${}^{15}\text{B}$. Beam extraction from the U-400M cyclotron will be upgraded to make this beam available.

^bThis beam is required for getting secondary beams of ${}^{24}\text{O}$ and ${}^{30}\text{Ne}$. The beam extraction upgrade indicated in footnote ^a will be required.

^cPrimary beam with such a high energy would be very efficient for RIB production at the proton dripline.

^dThis beam is required for getting secondary beams of ${}^{44}\text{S}$, ${}^{40}\text{Si}$, etc. The beam extraction upgrade indicated in footnote ^a will be required.

Table 8: RIB yields from a ^9Be production target with thickness optimised for the corresponding exotic nuclei. “Purity” is the part of the RIB of interest in the total secondary beam current. “Power” is power dissipated in the production target.

Primary beam	Energy MeV/amu	Intensity pμA	Second. beam	Energy MeV/amu	Intensity (pps) ACC	Intensity (pps) ACC-2	Purity (%)	Power (W)
^7Li	34	4	^6He	29	3×10^5	1×10^7	97	310
^7Li	34	2.5	^6He	24	3×10^5	1×10^7	97	200
^7Li	34	10	^6He	6	2×10^3	5×10^5	100	1350
^{11}B	32	10	^8He	26	2×10^4	2×10^5	92	720
^{11}B	32	10	^8He	11.5		2×10^4	95	1100
^{11}B	32	10	^9Li	25	2×10^5	4×10^6	70	800
^{11}B	32	10	^9Li	10		4×10^5	90	1700
^{15}N	49	10	^8He	40	2×10^4	2.5×10^5	92	400
^{15}N	49	10	^{11}Li	37	5×10^3	8×10^4	40	400
^{18}O	48	10	^{11}Li	37	2×10^3	8.5×10^4	35	2000
^{18}O	48	10	^{14}Be	35	1×10^2	4.2×10^4	50	1400
^{18}O	48	10	^{15}B	38	5×10^2	5×10^5	50	1400
^{36}S	49	10	^{17}B	35		1.5×10^2	4	5400
^{36}S	49	10	^{24}O	38		5×10^2	2	3800
^{36}S	49	10	^{24}O	38		2.5×10^2	20	3800
^{48}Ca	43	3	^{24}O	29		1.5×10^2	5	2000
^{10}B	39	10	^8B	31	5×10^4	9×10^6	25	400
^{10}B	39	10	^8B	31	5×10^4	5×10^6	90	400
^{16}O	43	10	^{13}O	32	5×10^2	6×10^5	70	980
^{20}Ne	53	10	^{13}O	37	5×10^2	5×10^5	70	1300
^{20}Ne	53	5	^{14}O	40	5×10^4	1×10^7	75	650
^{20}Ne	53	10	^{17}Ne	40	5×10^2	1×10^6	75	1300
^{32}S	52	10	^{24}Si	40		1×10^4	60	1450
^{32}S	52	10	^{27}S	38		1×10^3	60	1450